BOADI SAMSON
March, 2018

SUPERVISORS:
Dr. Caroline Lievens
Dr. Robert Hewson

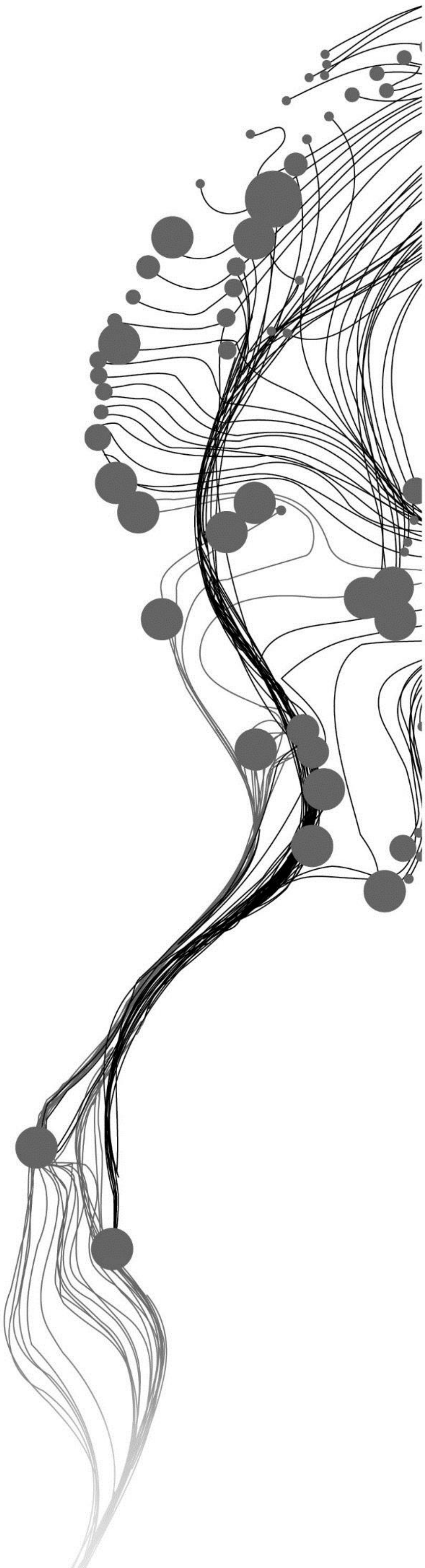

USING TERMITE MOUND GEOCHEMISTRY AND THE SPATIAL DISTRIBUTION OF THE MOUNDS TO SUPPORT SUBSURFACE IMAGING.

BOADI SAMSON
Enschede, The Netherlands, March, 2018

Thesis submitted to the Faculty of Geo-Information Science and Earth Observation of the University of Twente in partial fulfilment of the requirements for the degree of Master of Science in Geo-information Science and Earth Observation.
Specialization: Applied Earth Sciences

SUPERVISORS:
Dr. C. Lievens.
Dr. R.D Hewson.

THESIS ASSESSMENT BOARD:
Professor, Mark vd Meijde (Chair).
Dr. Mike Buxton (External Examiner, Technical University of Delft).

ABSTRACT

The depletion of near surface deposits has led exploration to focus on terrains with transported cover (sediments). The transported nature of the sediments makes it difficult to employ traditional methods such as soil sampling, and remote sensing, due to the issue of false geochemical anomaly. Geophysics, however, provides an excellent means to see beyond this transported cover. However, the cost of mobilisation and implementation makes it difficult for upcoming mining companies to implement, during the initial stages of exploration.

This study investigates the possibility of using the spatial distribution of termite mounds and their geochemistry to support subsurface imaging in complex regolith environment.

The spatial distribution of 1171 termite mounds was mapped using GPS traversing method. Statistical analysis (Autocorrelation, kernel density, and directional trend), was performed on the 1171-spatial distribution of the termite mounds using ArcMap 10.5.1. The resulting density map and the directional trend of the mounds were then superimposed on the aeromagnetic, chargeability and geological map of the research area.

Additionally, vertical cross-section of two (2) termite mounds and their immediate subsurface was sampled, both in the X, and Y direction, and ICP-OES, ASD, and XRD analysis performed on them.

The spatial distribution of the termite mounds was found to correlate with high magnetic anomalies and high chargeability zones. The termite mounds were found along most lithological contacts.

The termite mounds were found to have a similar trend to the major faults in the research area (NE-SW), a significant fault trend in orogenic terrains.Also, the geochemistry of the two selected mounds revealed the composition of the subsurface to be transported regolith, dominated by kaolinite. The kaolinite was found to be partially disordered, with an average crystallinity index of around 75 %.

The result indicates that the termite mounds are not randomly distributed. Their spatial distribution is influenced by accumulation of clay and moisture within faults, fractures, and dykes. The results additionally indicate that the geochemistry of the termite mound can be used to infer the subsurface composition of the regolith, and also the provenance of the clay mineral kaolinite could be related to semi residual environment, where mineralisation is related to the subsurface.

ACKNOWLEDGEMENTS

I wish to thank God for the opportunity to study here at the University of Twente.

I would also like to thank my supervisor's Dr Caroline Lievens and Dr Robert Hewson. You supported me greatly and were willing to help me throughout this research. You always tell me "look, Samson, it is your call, but….", This gave me the space to thoroghly consider this research to make it my own. I appreciate the immersive support and allowing this research to be a true reflection of me.

I would also like to thank Pelangio Resources for my access to their concession, provision of the geophysical imageries used in this research, and the support during my fieldwork. Not forgetting Dr Emmanuel Arhin of the University for Development Studies, for his encouragement and making my research with Pelangio Resources in Ghana possible.

My sincere gratitude goes to prof.dr. M. Van der Meijde for his support in the interpretation of the geophysical imageries. Not forgetting, Bart Krol and dr. F.J.A. Van Ruitenbeek, for their advice and support during this research.

In addition, I would like to thank UTS/ITC scholarship, and Theras Resources Sarl, for making my studies here possible.

To the lecturers at the University of Twente (ITC), I am grateful for equipping me with the required knowledge and skills to tackle this research. I would like to single out Dr. Chris Hecker and r.H.M.A van der Werff, for their encouragement, to take up this particular research.

Finally, I would like to thank my mum and dad Mr., and Mrs., Boadi for their support, prayers and encouragement during this research. To my aunty Gifty Owusu, my good friend Onallia Esther Osei and my girlfriend Sefakor Esi Kwawukume, thank you for your prayers and support. This would not have been possible without you.

TABLE OF CONTENTS

Abstract i
Acknowledgements ii
Table of contents iii
List of figures v
List of tables vi
1. INTRODUCTION. 7
1.1. Problem Definition. 7
1.2. Termites. 7
1.3. Termite Mounds. 7
1.4. Termite Bioturbation. 8
1.5. Factors affecting the Spatial Distribution of Termite Mounds. 8
1.6. Geophysics and the subsurface. 9
1.7. Geochemistry of termite mounds. 9
1.8. Research Objectives. 10
1.9. Thesis structure 11
2. STUDY AREA. 12
2.1. Study Area, Geological setting and Regolith. 12
2.2. Mineralisation. 13
2.3. Climate, Topography and Vegetation. 13
3. METHODOLOGY. 14
3.1. Fieldwork. 14
3.2. Laboratory Works. 14
3.3. Data, and Image processing. 14
3.4. Fieldwork. 14
3.5. Laboratory Works. 16
3.6. Data, and Image Processing. 18
3.7. Statistical analysis of termite mound distribution. 18
3.8. Spatial distribution of termite mounds on geophysical imageries, and geological map. 19
3.9. Geochemical Data treatment. 19
4. GEOSPATIAL RESULTS OF TERMITE MOUND DISTRIBUTION. 20
4.1. The Spatial distribution of termite mounds. 20
4.2. Spatial Autocorrelation 21
4.3. The density distribution of the termite mounds. 21
4.4. Directional trend within the termite mound distribution. 22
4.5. Drainage pattern within the research area. 23
4.6. The relationship between the directional trend of mound distribution and drainage. 24
4.7. The relationship between the directional trend of termite mounds and aeromagnetic. 25
4.8. The relationship between the directional trend of termite mounds and chargeability. 26
4.9. The relationship between the directional trend of termite mounds and major faults. 27
5. MINERALOGICAL AND GEOCHEMICAL RESULTS OF THE TWO SELECTED TERMITE MOUNDS. 29
5.1. Mineralogy of termite mound 1 and 2. 29
5.2. Crystallinity of kaolinite from termite mounds 1 and 2. 30
5.3. Mineralogy of termite mound 1 and 2 using (VNIR-SWIR-Spectroscopy) 32
5.4. Crystallinity of kaolinite from termite mound 1 and 2 (VNIR-SWIR- Spectroscopy). 32

5.5. Geochemistry of termite mounds 1 and 2. 33
5.6. Variation of the major elements and Gold (Au) within termite mound 1 and 2 and their subsurface. 35
6. DISCUSSION. 37
6.1. Spatial analysis of termite mounds. 37
6.2. Mineralogy and Elemental analysis of the two selected termite mounds. 42
7. CONCLUSION. 46
7.1. Spatial distribution of termite mounds. 46
7.2. Geochemistry of termite mounds. 46
7.3. Recommendation. 46
8. REFERENCES. 47
9. APPENDIX 51
9.1. Appendix 1 51
9.2. Appendix 1.1 51
9.3. Appendix 1.2 52
9.4. Appendix 1.3 52
9.5. Appendix 1.4 53
9.6. Appendix 1.5 53
9.7. Appendix 1.6 54

LIST OF FIGURES

Figure 1. Location and geology of study area. 12
Figure 2. Vegetation cover in the research area (Manfo-Ghana) 13
Figure 3. The location of the 1171 identified mounds and the two selected termite mounds 15
Figure 4.Sample location of termite mound samples. 16
Figure 5. Spatial distribution of termite mounds. 20
Figure 6. Shows the statistical analysis of the spatial distribution of the termite mounds, 21
Figure 7. The figure shows the density distribution of the termite mounds 22
Figure 8. The directional orientation of the spatial distribution of the termite mounds. 23
Figure 9. Surface drainage pattern within the research area. 24
Figure 10. The directional trend of termite mounds superimposed on the SRTM 25
Figure 11. The directional trend of the termite mounds distribution, superimposed on reduced to pole 26
Figure 12: The directional trend of termite mounds, superimposed on the chargeability 27
Figure 13. The directional trend of termite mounds superimposed on published major faults 28
Figure 14. XRD results of selected termite mound, and subsurface. 29
Figure 15. XRD results of selected termite mound, and subsurface. 30
Figure 16. XRD results of M12 (mound 1) and M7-2 (mound 2), 31
Figure 17. Modified after Artioli et al., (1995). X-ray powder diffraction patterns for two natural reference kaolinite samples: 31
Figure 18. M12 and M7-2 VNIR-SWIR spectra of termite mound samples from termite mound 1 and 2, 32
Figure 19. Variation of Mg within mound 1 35
Figure 20. Variation of Mg within mound 2 35
Figure 21. Variation of k within mound 1 35
Figure 22. Variation of k within mound 2 35
Figure 23. Variation of Al within mound 1 36
Figure 24. Variation of Al within mound 2 36
Figure 25. Variation of Au within mound 1 36
Figure 26. Variation of Au within mound 2 36
Figure 27. The directional trend of termite mounds and interpreted geology 39
Figure 28. Spatial density of termite mounds superimposed on the regional geology 40
Figure 29. The directional trend of termite mounds superimposed on the geology and Gold (Au) mineralisation, 41
Figure 30. K/Al vs Mg/Al ratio plot percent weight for subsurface of termite mound 2 45
Figure 31. The zoomed plot of the transported clay sediment quadrant, 45

LIST OF TABLES

Table 1. ICP-OES results of termite mound 1 and the immediate subsurface ... 33
Table 2. ICP-OES results of termite mound 2 and the immediate subsurface ... 34
Table 3. Statistics of selected major elements in % ... 34
Table 4. Statistics of major and trace elements in ppm ... 34
Table 5. Correlation matrix of gold, major and trace elements ... 44

1. INTRODUCTION.

1.1. Problem Definition.

Mineral exploration is imperative to locate new deposits. Civilization and society's prosperity depend on the continuous flow of minerals for development (Gandhi & Sarkar, 2016). Most countries' Gross Domestic Products (GDP) depends on the access to minerals, but current mineral resources are declining due to exhaustion of easily discoverable near surface deposits (Henckens et al.., 2016). The depletion of these near-surface deposits has led most exploration to focus on terrains with transported cover (sediments) exhibiting complexity in their regolith (Butt et al., 2000). Exploration in such complex regolith environments with remote sensing and traditional methods such as soil sampling and pattern drilling has not always proved successful (Arhin E., 2009). This situation has led most geologists to map the subsurface in such terrains with geophysical methods such as aeromagnetic, Induced Polarisation (IP) resistivity, among others. This approach, however, is costly during the initial stages of exploration. Hence the need for investigating the geochemistry of termite mounds and their spatial distribution as an alternate tool to support subsurface imaging of the regolith in terrains with transported cover, dominated by termite mounds.

1.2. Termites.

Termites are eusocial insects that live either in the Earth (Subterranean), or on trees and dry wood (Arboreal). They are considered as destructive insects; destroying farm produce and eating dry woods of building (Obi et al., 2008). Termites that destroy farm produce are the subterranean termites. Subterranean termites build large earthen structures on the surface of the earth, as their habitat. They sample the subsurface materials to build the mounds. They are therefore referred to as soil engineers; vertically transporting and altering organic and inorganic materials (Chakravarthy & Sridhara, 2016), in the form of lithic fragments to construct their mound. Minerals and elements make up the lithic fragment. The movement of these lithic fragments from their microenvironment to the surface enhances the mobility of elements and enhance some key geochemical indicators within the subsurface (Anand et al., 2016). The mobility of these elements and minerals mainly by termite workers are most dominant from the Phreatic (above the water table) zone and within the arid to the semi-arid regions of the world. Termite workers move large quantities of soil from different horizons to build the mound.

Termites abide by social hierarchy. Therefore, labour within the mound is divided among the workers, soldier and the producers (Eggleton, 2010). The soldiers defend the colony against invaders, while the producers continually reproduce new species of termites. Several species of termites have been identified in the world. Eggleton, (2000) describes 2600 species of termites worldwide, out of which 660 species was attributed to the African continent. Out of the 2600 species, 86 have been reported by Forsyth, (1966), in Ghana, which is made up of 38 genera, and comprises of mound building and dry wood termites.

1.3. Termite Mounds.

Termite mounds are narrow or conical Earth structures built by subterranean termites. These structures extend several meters beyond the Earth subsurface. Termites from the family *Macrotermes*, build mounds with materials only from the deep-seated environment within the earth (Harris, 1956). Termite mounds can have several shapes depending on the climate, the availability of resources; clay and moisture, and also the species within a colony (Harris, 1956). For instance, termite species *Macrotermes natalensis* builds the cathedral type of mound (Turner, 2000). Termite mound architecture can be associated with termite species, but different species of termite could build similar mounds based on adaptation strategies (Harris, 1956). Termite mounds can be classified into magnetic, cathedral, conical, mushroom or collapsed types. Some of these mounds, for example, the magnetic mounds, have unique characteristics; being oriented in the north-south direction towards the magnetic north (Grigg et al., 1977).

1.4. Termite Bioturbation.

Termite workers transport subsurface materials to the surface. Termite's workers can burrow to the subsoil, beyond the transported cover, contributing to the development of the soil (Lobry et al., 1995; Sako et al., 2009; Watson, J. A.L., 1970). In particular, termite workers transport subsurface materials in the form of rounded pellets, conserving the micromorphology of the excavated horizon (Cosarinsky, 2011). These rounded pellets can sometimes contain traces of ore body associated "indicator" minerals and elements, which are sometimes masked by the transported cover (Anand et al., 1993; Butt et al., 1997). For this reason, termite mounds have been used as a geochemical sampling medium in complex regolith environments, revealing mineralisation under cover and in shallow sediments (Gleeson et al., 1989; Prasad et al., 1984). High concentrations of clay minerals such as kaolinite and illite have been reported in termite mounds (Hesse, 1955; Sako et al., 2009). According to Harris, (1956), Termites preferentially sample clay minerals to construct the chamber where the queen termite lives.

Termites can burrow up to several meters below the earth surface. According to Coventry et al., (1988), termites can burrow up to depths of 70 m, below the earth surface transporting materials to construct their mounds. The termites that burrow deep and vertically transport subsoils can be evident from the mineral composition of their nest. Liu et al., (2007); Sako et al., (2009) observed the presence of smectite, muscovite, illite, and carbonate within termite mounds constructed with subsurface materials.

1.5. Factors affecting the Spatial Distribution of Termite Mounds.

Although termites burrow several meters below the earth surface, they cannot tunnel within and extract material from hard rock (Mège & Rango, 2010). They, therefore, build tunnels in already existing geological structures such as weathered dykes and fractured/sheared fault zones (Mège & Rango, 2010). These geologic structures can sometimes contain clay or moisture, which is an essential resource for the construction and maintenance of the mound (Harris, 1956). The presence of these clay or moisture can sometimes influence the spatial distribution of the mounds. The termites, therefore, assume a preferential path along these structures for easy accessibility to resources (clay and moisture), making them align their mounds either along or across such geologic features. An example is an alignment of termite mounds along a dolorite dyke, reported by Mège & Rango, (2010) in Ethiopia.

Termites mound distribution can be influenced by the presence or absence of clay and moisture in the subsurface. These resources sometimes accumulate in dykes and paleochannels (Samadder et al., 2011). According to Babiker & Gudmundsson, (2004), dykes are preferred pathways for groundwater recharge. Dykes serve as storage for groundwater in the dry season (Mège & Rango, 2010). Subterranean termites build their mounds on the soil surface, often in areas of increased moisture (Davies et al., 2015). This helps them to maintain the humidity of their mounds (Harris, 1956). Termite mounds distribution can sometimes be influenced by the presence or absence of these resources Mège & Rango, (2010). Termites typically search for moisture and clay and in the process transport earth materials to the surface, possibly from such weathered dykes.

Old buried river channels (paleochannels) can sometimes be associated with areas of increased moisture and can hence also be a potential target for termite activity. Paleochannels are old river channels, buried within the current landscape (Singh et al., 2011). These channels sometimes contain graded sedimentary deposits of very fine silt or clay materials, and permeable deposits which make them a potential source for groundwater recharge (Samadder et al., 2011).

Termites in search for clay and moisture construct mounds that can sometimes reveal these old buried channels. It is believed that the spatial distribution of termite mounds is influenced by some geological features, hence analysing the spatial pattern of these mounds could be used to reveal such overlain subsurface properties.

1.6. Geophysics and the subsurface.

Geophysical prospecting complements traditional methods to gather subsurface information (Jayawickreme et al., 2014). This information could be weak zones such as fractures, dykes, faults and geological contacts (Hinze et al., 2013). There are several techniques in geophysical prospecting to collect this subsurface information. These techniques are Aeromagnetic, Resistivity, and Electrical chargeability (Hinze et al., 2013).

The aeromagnetic technique aims at investigating the subsurface. This technique images the subsurface based on variations in the earth magnetic field. The earth magnetic field is influenced by different rock types (Hinze et al., 2013). Different types of rocks exhibit different magnetic intensities depending on the magnetite content of the rock type and its environment of formation (Mariita, 2010). For example, dykes, fault contacts between different units and basalts from variable lava flow also cause magnetic anomalies.

Resistivity technique determines the apparent resistivity of subsurface features. Resistivity is conducted either in profiling or sounding mode depending on the aim of the survey. In the sounding mode, subsurface features are mapped and change horizontally with respect to depth. Profiling mode maps subsurface features with respect to lateral extension. In both processes, small electrical current is passed into the earth to measure the apparent resistivity (Jackson, 1975).

Electrical chargeability is a function of induced polarisation (IP resistivity)(Park et al., 2017). In geophysics, chargeability is used to characterise the subsurface based on the accumulation of charges in the earth surface under the influence of electrical current(Park et al., 2017). The chargeability of the subsurface could be attributed to either disseminated or massive sulphides, mafic rocks, and clay minerals, (Telford & Sheriff, 1990).

Despite the strengths of geophysics, it has its challenges. Geophysics provides an excellent means to look beyond the earth surface. The various geophysical methods tend to interpret the subsurface through modelling. The techniques involved are complex and requires well-trained personnel to give a proper interpretation of the subsurface information. The cost of mobilisation, and operation is also of concern. According to Pelangio Resources (Personal communication), the cost and mobilisation of geophysics raise the cost of exploration. Also, according to M. Costelloe, of the Australian Society of Exploration Geophysics, (email communication, 1/17/2018), the cost of mobilisation for in particular, aeromagnetic exploration using helicopter system is around 20,000 Australian dollars, while the cost of the investigation is estimated to be 20 Australian dollars per line km.

1.7. Geochemistry of termite mounds.

Geochemistry of soil samples is one of the traditional primary methods in mineral exploration. In mineral exploration, the application of geochemistry in complex regolith environment has produced mostly false anomalies (Anand et al., 2016). Recently, the geochemistry of termite mounds has gained popularity in complex regolith environments because of its success in locating hidden deposits (Affam et al., 2005). The geochemistry of termite mounds has been used to locate hidden ore deposits and associated pathfinder elements in several environments. For example, Arhin et al., (2015) used termite mound geochemistry to establish pathfinder elements in complex regolith environment in Ghana. Sako et al., (2009), reported elevated levels of rare earth and trace elements in termite mounds in Namibia. Le in (1991) used the geochemistry of the mounds to locate uranium deposit in a lacustrine paleochannel, 25 meters beneath the surface. Termite mound geochemistry has been proven useful to locate metal deposits (Kebede, 2004), but there are not enough studies on characterising the subsurface mineralogy and regolith using the mound geochemistry.

1.8. Research Objectives.

1.8.1. Main objectives.

The primary purpose of this research is to attempt to interpret the subsurface using termite mound geochemistry, and the spatial distribution of the mounds in Manfo-Ghana.

1.8.2. Specific objectives.

1. To use termite mound geochemistry to infer or characterise the subsurface
2. To map and analyse the spatial distribution of termite mounds within the study area using GPS traversing.
3. To map subsurface features such as paleochannels and dykes, via geophysical imagery and determine the relationship between the inferred subsurface features and the spatial distribution of termite mounds within the study area.
4. To determine the provenance of clay minerals (e.g. Kaolinite) within the termite mounds and their possible relationship to alteration or regolith processes.

1.8.3. Research questions.

1. Can termite mound geochemistry be used to infer the subsurface elemental and mineral composition?
2. Can the elemental and mineralogy of the termite mounds be used to deduce the nature of subsurface geology/regolith?
3. Does the spatial distribution of the termite mounds follow a particular pattern?
    - Can the spatial distribution pattern of termite mounds be used to infer weak geological zones such as lithologic contacts and dykes in the study area?
4. What is the provenance of clay minerals in termite mounds?
    - Are clay minerals related to transported or relict environments?

1.8.4. Hypotheses.

1. Termite mound geochemistry can be used to infer the subsurface regolith.
2. Termite mounds are randomly distributed within the study area.
3. Spatial distribution of termite mounds can be used to infer the presence of subsurface features such as dykes, and paleochannels.
4. Altered clay minerals (e.g., Kaolinite) within termite mounds are associated with sub-surface regolith.

1.9. Thesis structure

The thesis has been organised into five chapters. Chapter 1, Introduction, defines the research problem leading to the research objectives, research questions, and hypotheses. Chapter 2, talks about the study area selected and review the relevance to the studies. This includes the climate, topography, vegetation, mineralisation, geological setting and the regolith. Chapter 3, Methods and data, explains the methodology followed to carry out the research, from fieldwork, deskwork; geochemical data treatment and analysis and termite mound spatial maps. Chapter 4, Geospatial results, present the results of the geospatial analysis of the termite mounds distribution. Chapter 5 Mineralogical and geochemical results of the two selected termite mounds. Chapter 6, Discussion, presents the interpretation of the geospatial results, including the mineralogy and geochemistry of selected termite mounds. Chapter 7, finally presents the conclusion and recommendations.

2. STUDY AREA.

This chapter talks about the study area; geology, regolith, mineralisation, and the climatic condition.

2.1. Study Area, Geological setting and Regolith.

The location of the study area is in Southern Ghana. It is along the north-central portion of the Hercynian structurally trending Paleo Proterozoic Sefwi Bibiani gold belt of Ghana (Schlüter, 2006). Shown between the coordinates of 2°19'58.966"W 6°52'28.876"N from the north and 2°14'59.352"W 6°48'59.78"N to the south, see Figure 1. The study area covers a total area of 65 square km. The area represents one of the most significant Proterozoic gold belts in the world (Allibone et al., 2004). Birimian meta-volcanic, meta-sediments, mafic volcanic and small granitoid bodies underlie the study area (Nude et al., 2014). To the east, a major northeast-trending fault traverses the study area ("Mineral Resource Evaluation Technical Report, Manfo Gold Project," 2013). The study area has undergone some form of modification of the regolith, with formation of laterite caps. Earlier studies by Nude et al., (2014) shows that surface dispersion processes have displaced some soil geochemical anomalies relative to mineralised bedrock. This has led to the issue of false geochemical anomalies in the surficial regolith. Soil geochemical response within the research area was found to be unrelated to the underlying mineralisation, during test drilling ("Mineral Resource Evaluation Technical Report, Manfo Gold Project," 2013). Careful analysis of the study area shows that transported depositional sediments overlay some geological units as evident from rounded to sub-rounded lithic fragments within the regolith (Nude et al., 2014).

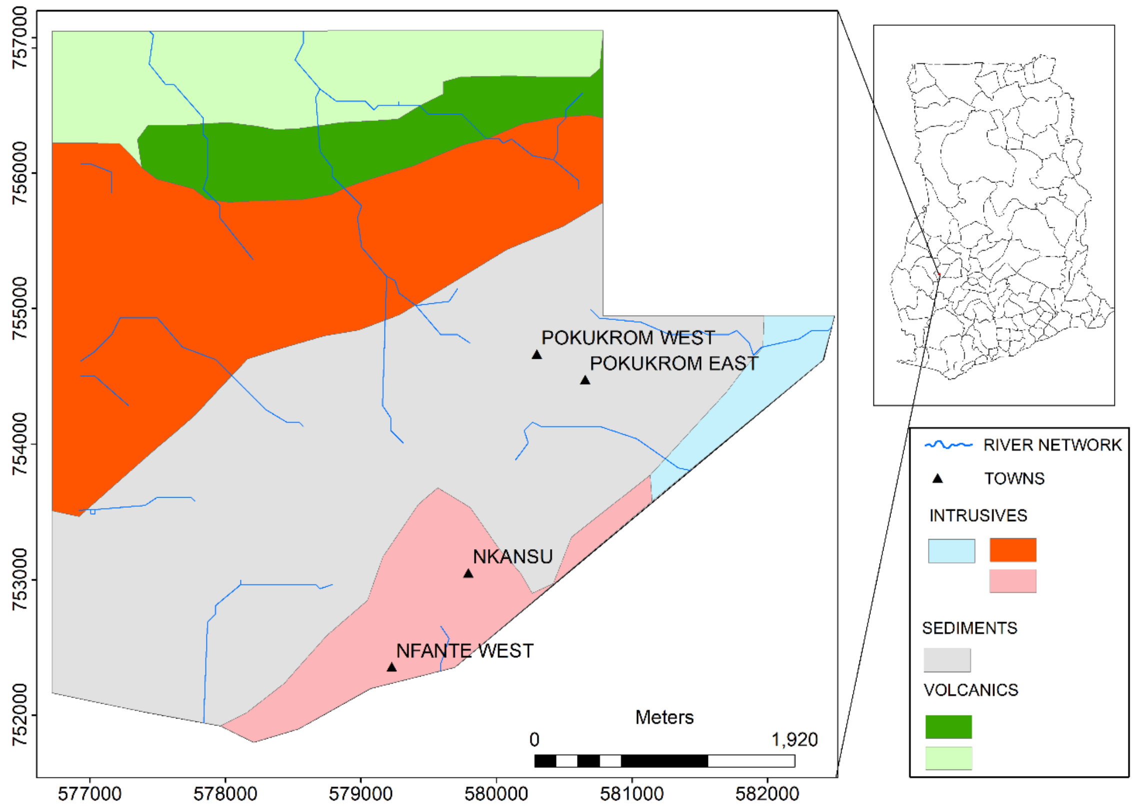

Figure 1. Location and geology of study area. Interpreted from a 1:200000 geologic map of Manfo/Akroma. Datum WGS 1984, zone 30N.

2.2. Mineralisation.

Mineralization in the study area is a structurally controlled orogenic deposit, localised along a significant northeast-striking fault zone, referred here to as the Sefwi Bibiani fault zone. This fault system restricts the mineralisation. Gold mineralisation in the research area is associated with broad zones of pervasive to fracture-controlled quartz-sericite-carbonate-pyrite alteration. This overprints hematite alteration hosted predominantly in sheared and locally brecciated, altered granitoid rocks, and to a lesser extent brecciated hematite-altered mafic metavolcanic rock (Consulting, 2013).

2.3. Climate, Topography and Vegetation.

The climate of Ghana is tropical with distinct wet and dry seasons. Dry seasons are from November to February and, in the south, briefly in August. The area experiences rain from March to July and September to November (Norgrove & Hauser, 2015). Annual precipitation ranges from 700 to 2,100 millimeters, and daytime high temperatures go from twenty-seven to thirty-seven degrees Celsius. The study area comprises of sporadic low hills isolated by generally expansive valleys ranging between 190 and 280 meters above sea level. A semi-deciduous jungle forest describes the vegetation in the research area (Counseling, 2013). The predominance of vegetation in the examination zone makes it difficult to utilize satellite images, for example, ASTER in the study area see Figure 2.

Figure 2. Vegetation cover in the research area (Manfo-Ghana).

3. METHODOLOGY.

This section entails the methods used. These include data processing, fieldwork and laboratory work. First, a brief introduction of the various methods, followed by detailed methodological approaches for the deskwork, fieldwork and laboratory work.

3.1. Fieldwork.

The fieldwork includes preliminary ground truthing of previously supplied gridded geophysical image anomalies, detailed photography of the surface geology, vegetation cover and landforms. Additionally, the spatial distribution of termite mounds was mapped with the help of a global positioning system (GPS). The vertical cross-section of two selected termite mounds and the subsurface in their immediate environments was finally sampled. The selection of the two termite mounds was based on high and low anomalous zones in the aeromagnetic imagery, possibly related to mineralised dykes or magnetic body and non-magnetic bodies respectively. Details of the fieldwork can be found in section 3.4.

3.2. Laboratory Works.

The vertical cross-section samples of chosen termite mounds and their immediate subsurface were digested via tetraborate fusion, and the elemental composition determined via Inductively Coupled Plasma Optical Emission Spectrometer (ICP/OES). The vertical cross-section samples of the selected termite mounds and their immediate subsurface: the mineralogy via X-ray diffraction (XRD) and Terraspec ASD-Halo. Details of the laboratory works can be found in section 3.5.

3.3. Data, and Image processing.

The data and image processing include mapping of surface drainage using Shuttle Radar Topographic Mission (SRTM) data. Additionally, the spatial distribution of termite mounds was accessed. Furthermore, subsurface features such as dykes, faults, geological contacts, and other weak structures within the subsurface were interpreted from geophysical imageries (e.g. aeromagnetic, chargeability) supplied by Pelangio Resources. The interpretation of the various geophysical imagery was performed, and possible structures delineated. Also, statistical analysis was performed on the ICP-OES analytical results of the samples extracted from the two termite mounds and the subsurface. Details of the data and image processing can be found in section 3.6.

3.4. Fieldwork.

Preliminary ground truthing of the interpreted streams from the SRTM data was performed. Ground truthing the geophysical imageries; aeromagnetic and chargeability was not possible at this stage of the research because of thick regolith cover, which hindered the exposure of outcrops. The spatial distribution of termite mounds within the research area was mapped, using GPS traversing Figure 3. GPS coordinates of termite mounds were recorded in a gridded pattern with an eTrex 30x GPS. The GPS reading of each mound was recorded with an average accuracy of 3 meters. The GPS reading represents point measurements of the mounds.

Description of the termite mounds was performed, this includes the colour, whether the mound was active or inactive, presence or absence of lithic fragments, among others. Also the locality name of each termite mound was indicated. About 1171 termite mounds with their GPS coordinates were recorded. Detailed photography of the mounds was also taken.

Two termite mounds were selected from the 1171 mounds for detailed sampling. The decision to sample a particular mound was based on the spatial distribution of the mound on the aeromagnetic imagery. Mound one (M1) was selected from a low magnetic anomalous zone, possibly related to surfacial sediments whiles mound two (M2) was from a high magnetic anomalous zone possibly dyke related, see Figure 3. Also according to Pelangio resources (http://www.pelangio.com/s/manfo.asp?ReportID=689206), gold-bearing intervals are immediately adjacent magnetic metasediments or volcanics, within the research area.

Vertical cross-section of the two selected mounds and the subsurface in the immediate environment of the mound were undertaken. Sampling interval of 0.5m along and across the mound was carried out, from the top of the mound to the bottom, both in the X and Y direction. Also, a sampling interval of 0.5m was conducted within the subsurface (see Figure 4). The depth of the vertical cross-section of the subsurface depended on the height of the mound above ground, as indicated by Arhin & Nude, (2010), the height of termite mound is proportional to its depth. It is worth noting that control sample from the environment on the mound was not sampled.
A total of three weeks was involved in the field work, which includes mapping of the spatial distribution of the mounds, and sampling the vertical cross-section in two mounds and their immediate subsurface.

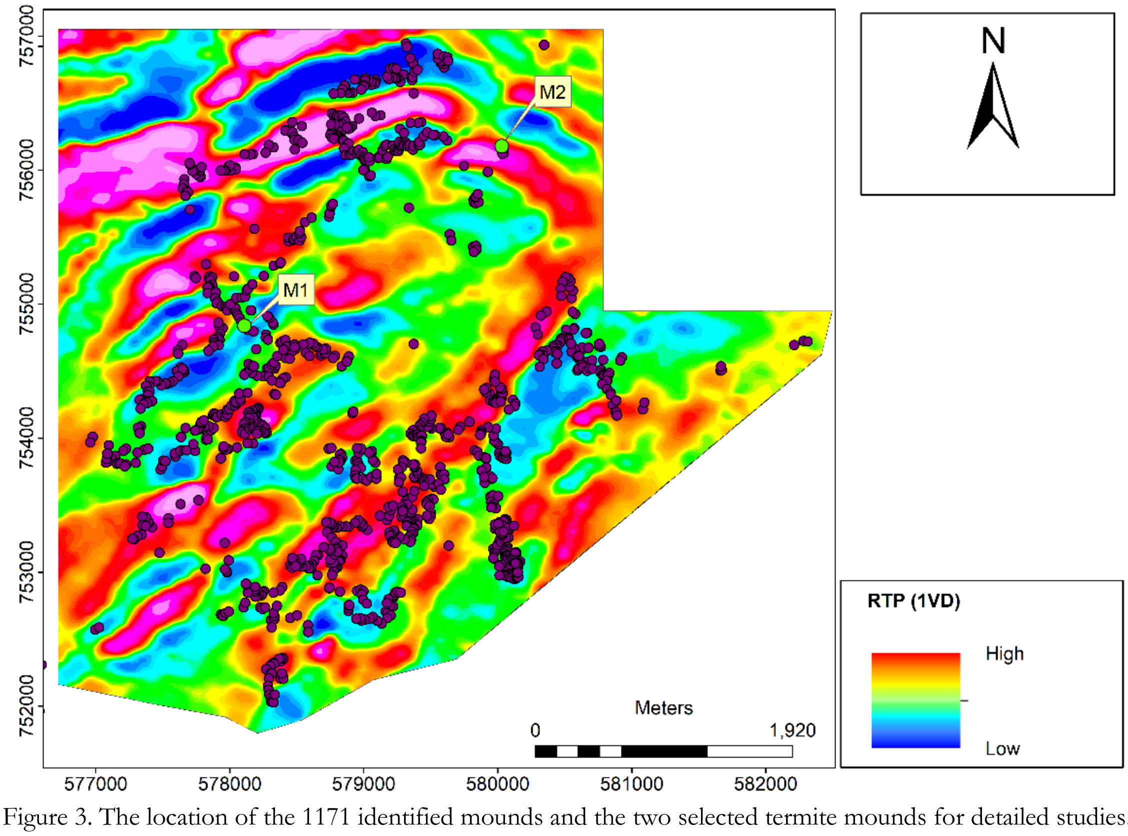

Figure 3. The location of the 1171 identified mounds and the two selected termite mounds for detailed studies. ("M1" Non-anomalous/sedimentary, anomalous zone, "M2" anomalous zone, dyke related overlying aeromagnetic).

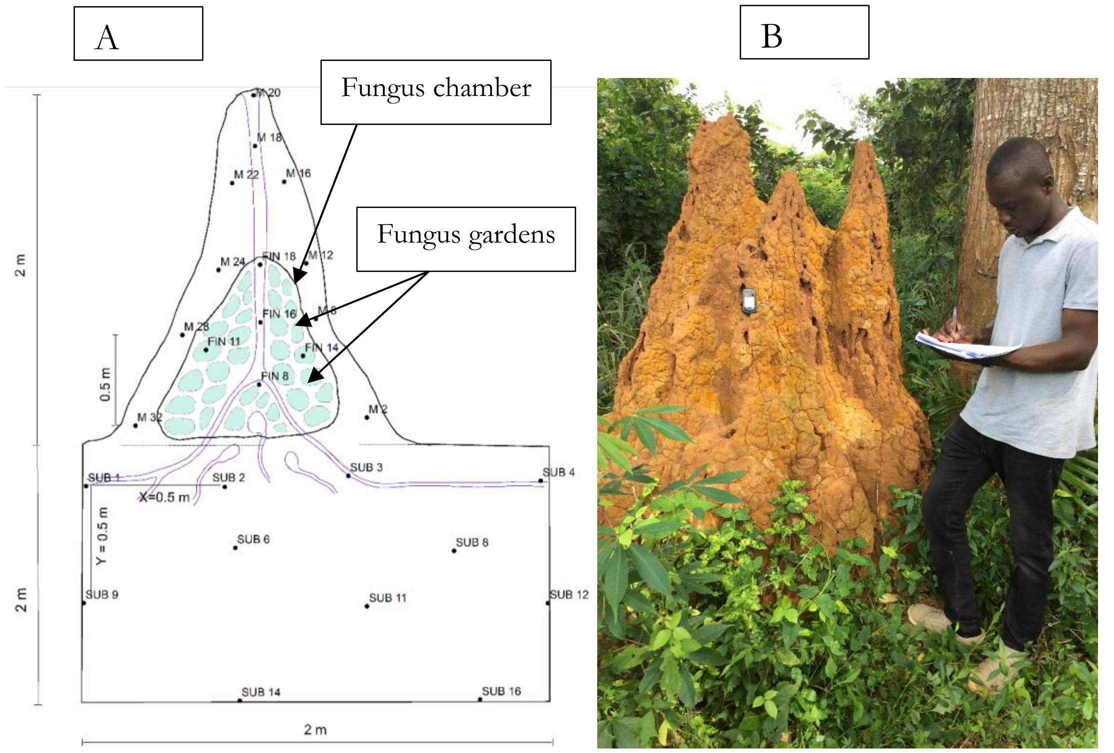

Figure 4.Shows the sample location of termite mound samples (A), and mapping the spatial distribution of termite mound using GPS traversing method (B).

3.5. Laboratory Works.

3.5.1. Solids sample preparation for ICP_OES analysis.

Solid termite mound samples and the subsurface samples was converted to a powdered form, ready for fluxing, fusion and ICP-OES analysis, following standard of operation by (Sandström, Reeder, & Bartha, 1998).

- 29 representative samples were selected from the subsurface, and also from the mound. This selection was performed for each of the two mounds and the subsurface separately.
- The selected termite mound and subsurface samples were oven dried at 105 °C for 24 hours.
- A desiccator was used to cool the samples and milled in a Retsch pulveriser.
- The pulverized samples were sieved for a fraction finer than 250 microns.

3.5.2. Sedimentation of selected samples for XRD analysis.

Sedimentation is a process of segregating different fractions of soil particles, based on gravity. The sedimentation was done to separate the clay fractions from the termite mound soil sample. This is because visually, quartz was seen to be dominant in the sample, which may influence the intensity of the clay mineral diffractogram, making it difficult to access the crystallinity of the clay minerals. A method proposed by Jackson (1956) was used in the sedimentation process, followed by clay content determination using the pipette method (Van Reeuwijk, 2002).

- 20 grams of 2 selected milled samples <250 microns was placed separately into two flasks.
- 1000 millilitres of Millipore water was added to the sample in the flask.
- The sample was then thoroughly shaken to mix with the Millipore water.
- The sample was left to settle by gravity and monitored for 15 minutes.
- 200 millilitres of suspended sample was then pipetted each from the sample solutions into two separate beakers.
- The beakers were then placed in an oven of temperature 105 degrees Celsius to dry.
- Dry sample was then collected onto separate petri-dish for XRD analysis.

3.5.3. Elemental analysis using Perkin Elmer 8300DV ICP-OES.

The distribution of elemental concentrations in termite mounds was calculated after the tetraborate digestion of the termite mounds and subsurface cross-section samples. For the tetraborate fusion, 0.1g of passing fraction of termite mound samples and the subsurface samples was weighed separately in platinum beakers and mixed with a tetraborate mixture (flux) of 1 g each. The samples were then fused at 1200 °C into pellets. The obtained pellets were dissolved in 50mL of nitric acid (HNO_3) (69%, Suprapur, Merck) into a clear solution. Following this process, the solutions were then analysed with ICP/OES for multi-element and gold. The multi-elemental composition including gold was then quantified relative to a reference standard for the multi-element and gold (Au) separately. All digestions were performed in duplicates and the results corrected with blank experiments.

3.5.4. Mineralogical Analysis using X-Ray Diffraction method.

The XRD analysis was performed on the passing fraction of termite mounds and the subsurface samples, using a Bruker D2 Phaser XRD. The sample powder is put in an XRD sample holder (approximately 1 gram) and is analysed in the XRD. The X-ray source is Cu Kα at 30 kV and 10 mA with a divergent slit of 1 mm, a detector slit of 8 mm and a knife to prevent backscattering 1 mm above the sample. The XRD patterns were obtained from 6° to 80° (degrees 2θ), with steps of 0,012° and each step for 0.1 seconds. The measurements were carried out repeatedly per sample to reduce background noise until the diffractogram had an adequate resolution to perform semi-quantitative analysis. The diffractogram was then analysed using DIFFRAC.EVA (https://www.bruker.com/applications/material-science.html) and compared to a database with diffractogram of pure mineral phases. The semi-quantitative interpretation was also performed using DIFFRAC.EVA.

3.5.5. Mineralogical Analysis using ASD- VNIR- SWIR Spectroscopy.

The ASD-Terraspec Halo (https://www.asdi.com/products-and-services/terraspec) were used to identify minerals in both near infra-red (NIR) and short wave infra-red (SWIR) range (0.45-2.5 um) of the spectrum. The ASD- Terraspec Halo was used to analyse the prepared samples used in the XRD analysis, taking into account, the influence of grain sizes on the resulting spectra. The prepared samples were measured with consistent observation geometry. Dark-current and white reference measurements were performed in between measurements, to remove background noise and to calibrate the reflectance. Spectral reflectance measurements were then recorded and further analysed using Envi 5.1(http://www.harrisgeospatial.com) to identify the individual minerals. The analysis of the pulverised samples could reduce the intensity of the spectra, (Erdemoğlu & Baláž, 2012), as stated earlier. This effect was considered in the interpretation of the spectra results.

3.6. Data, and Image Processing.

3.6.1. Extraction of current streams (SRTM).

Current drainage pattern within the research area was inferred in ArcMap 10.5.1 (ESRI) from SRTM with 30-meter resolution digital elevation model (DEM) downloaded from Earth Explorer (https://earthexplorer.usgs.gov/). The Hydrology tool in ArcMap was used to infer the probable locations of streams from the SRTM image, after which the spatial extent of the interpreted drainage area determined.

3.6.2. Termite Mounds Geo-Spatial Mapping.

The spatial location of the termite mounds was plotted in ArcMap 10.5.1. The spatial distribution of the mounds was then analysed using various spatial statistical analysis (spatial autocorrelation, kernel density and standard deviational trend analysis) to determine the areal density of the mounds and structural trends within the distribution of the mounds in the research area. Details of the statistical analysis can be found in section 3.7.

3.7. Statistical analysis of termite mound distribution.

3.7.1. Spatial Autocorrelation (Moran's I global autocorrelation).

The Moran's I global autocorrelation is an inferential statistical approach that analyses the overall spatial correlation (similarity) of a data set based on the spatial location of the data, and its attributes (Moran, 1950). The Moran's spatial autocorrelation evaluates whether a distribution is clustered, dispersed, or random. The Moran's spatial autocorrelation calculates the Moran's Index, a Z-score and a P- value. A Moran's Index of -1, 0 and 1 indicates perfect dispersion, perfect randomness and perfect clustering respectively (Zhou & Lin, 2008). The P-value and the Z-score are used to evaluate the significance of the Moran's Index. Lower P values and positive Z scores indicate that the Morans Index (I) is significant, whiles higher P values and negative Z scores indicate non-significance in the Moran's Index (Bhunia, Kesari, Chatterjee, Kumar, & Das, 2013).
The termite mounds were plotted within the research area in ArcMap 10.5.1, with the appropriate projections (WGS 1984). Spatial autocorrelation within the spatial statistics toolbox; analysing patterns in ArcMap was invoked. The spatial distribution of the mounds was used as the input feature, and the mounds locality name generated on the field, e.g. Pokurom-east and Pokukrom-west, coded into numerical values, e.g. 0 and 1, and used as a distance decaying factor to the input field. The spatial autocorrelation between the objects was then conceptualised using the inverse distance relation, where objects close to each other is much more related than objects farther away (Tobler, 1970). The Euclidean distance method was used as a measure of distance between the termite mounds; this method assumes a linear distance between any two mounds (J.C. Gower, 1985). A report of the spatial autocorrelation was then generated.

3.7.2. Density distribution of termite mounds using kernel density.

The kernel density distribution tool calculates the magnitude of features per unit area (Silverman, 1986). The tool uses a kernel function to fit a smooth surface to each feature. The plotted termite mound was used for this analysis. The kernel density distribution tool, within the spatial analysis tool in ArcMap 10.5.1 was used for this purpose. The termite mound plot was used as the input feature to the kernel density tool. The attribute field representing similarities within the mounds (coded locality name) section 3.7.1 was used as the population field. The planar method of distance measurement was used to determine the distance between any two termite mounds in a straight line, since the area in consideration is not large, and coordinate system (WGS 1984) is appropriate for linear distance measurement (Kennedy, 2013). An output map of the predicted density of termite mounds in square kilometres was then derived.

3.7.3. The directional trends of termite mounds.

The spatial distribution of the termite mounds was used as an input feature to the directional distribution tool (ArcMap 10.5.1). The size of the output ellipse was set to 1-standard deviation, to encompass 68 percent of the distribution (Bland & Altman, 1996). The distribution was then weighted by the location in the X and Y direction, to restrain the trends within the locations of the termite mounds.

3.8. Spatial distribution of termite mounds on geophysical imageries, and geological map.

The spatial distribution of the termite mounds was superimposed on the geophysical imageries; aeromagnetic and chargeability. The aeromagnetic image used here has a 100-meter flight spacing, gridded to 20 meters cells. The aeromagnetic data has further been reduced to the magnetic pole, to align the magnetic anomalies over the sources of the anomalies, e.g. dykes. Finally, a first vertical derivative (1VD) filtering applied, to filter high-frequency electromagnetic anomalies, and map shallower features such as dykes and other magnetic bodies (Warren et al., 2016). The chargeability imagery used here is a ground-based time domain, with a 20-meter gridded resolution.

The chargeability image maps possible sulphide deposits, either disseminated or fracture filled. Lineaments that could be related to subsurface features were inferred from the geophysical imagery. The spatial distribution of the termite mounds was then superimposed on the geophysical imagery and inferred lineaments, to establish the relationship between the mound and any possible subsurface features. The spatial distribution of the termite mounds was also superimposed on the mapped lithologies to analyse the relationship between the mounds and the lithologies, including the lithological contacts and faults (Pelangio Resources, 2015).

3.9. Geochemical Data treatment.

The geochemical data was carefully examined with a statistical treatment, to obtain a data, fit for the interpretation. It was observed that one crucial element, potassium (K), which is essential for the classification of the mound material was below the detection limit of the analytical method, in the two mounds, except in three samples, and the subsurface of termite mound 1. The element K, below the detection limit, does not mean that the element is not present in the sample, but may be present at very low levels, which requires a more sensitive method to be able to detect it. As proposed by Croghan, (2003), when the element K is below the detection limit (DL) of 0.005 ppm of ICP-OES, it can be replaced by (0.005ppm) $* \sqrt{2}$. The K values below DL was then replaced by (0.005ppm) $* \sqrt{2}$. The concentrations of the major elements (aluminium, potassium, magnesium, iron, calcium) in part per million (ppm) were converted to percentages, by multiplying the concentration of the element in ppm by 0.0001. This was done to get the weight percent of the metals for classification of the mound samples. A method proposed by McQueen, (2006), for unravelling the regolith, using the ratio of the relative mobile elements magnesium, potassium and the relatively immobile element aluminium, was applied, that is Mg/Al and K/Al in weight percent. A scatter plot was generated from the resulting ratios, with Mg/Al on the Y-axis and K/Al, on the X-axis.

The relationship between gold (Au), major and trace elements was determined, using factor analysis in SPSS statistical software version 24 (http://www-01.ibm.com/support/docview.wss?uid=swg24041224). Factor analysis reduces the complexity of a data set, which helps to reveal the elemental association within the data set. Gold was used as a target element to the major and trace elements. The principal component (correlation matrix) analysis was used to extract the factors, within the dataset. An eigenvalue of 1 was defined, and used as a threshold, to help extract all factors with an eigenvalue greater than 1. Also, an orthogonal rotation was applied to the dataset to help extract maximum factors.

4. GEOSPATIAL RESULTS OF TERMITE MOUND DISTRIBUTION.

4.1. The Spatial distribution of termite mounds.

Figure 5 below shows the spatial distribution of the termite mounds within the research area. From the figure, it could be seen that the termite mounds trend linearly in the north-east direction (Hercynian), both in the south-east and the north-west of the research area. From the southeastern portion of the research area, a north-northwest trend (A-A) is observed. This new trend is almost at right angle to the general Hercynian trends within the research area. To the north of the research area, the termites form a semi-circular trend. Some of the mounds could be seen clustered at portions of the research area; whiles others are isolated. These trends indicate that a spatial factor influences the distribution of the mounds. Detailed discussion can be found in section 6.1.1.

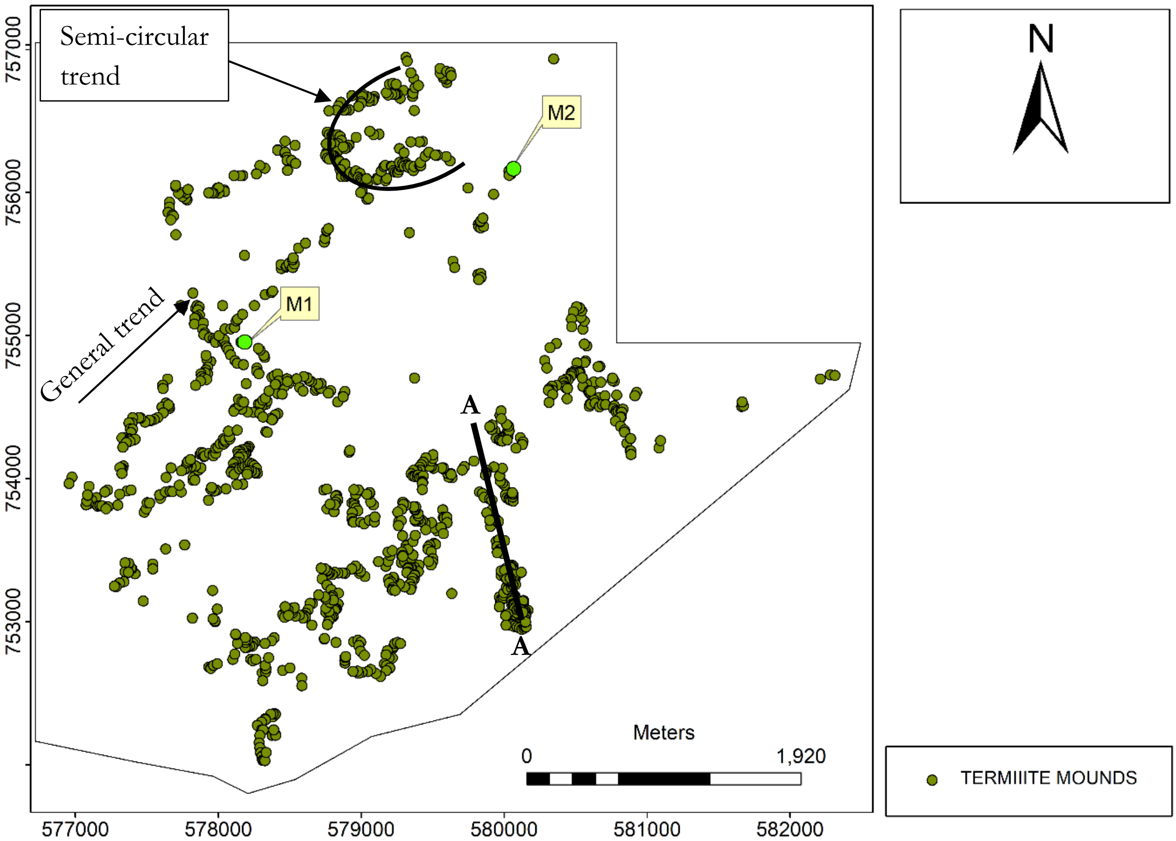

Figure 5. Spatial distribution of termite mounds. Showing circular termite trend within the northern portion of the research area.

4.2. Spatial Autocorrelation

Statistical analysis of the termite mounds using Moran's I global autocorrelation was performed in ArcMap 10.5.1. The Moran's I global autocorrelattion was used to determine whether the termite mound distribution is clustered, dispersed or random, which will help to determine if there is any underlying spatial pattern within the termite mound distribution. The statistic was performed on 1171 termite mounds from the research area. A null hypothesis, assuming the distribution within the mounds to be random was set. The result is presented in Figure 6. The result returned a Moran's Index of 0.62, P value of 0.00, indicating a P value <0.001, a positive Z score of 59.75, and a critical value greater than 2.58. The P value indicates that statistically, the result is highly significant.

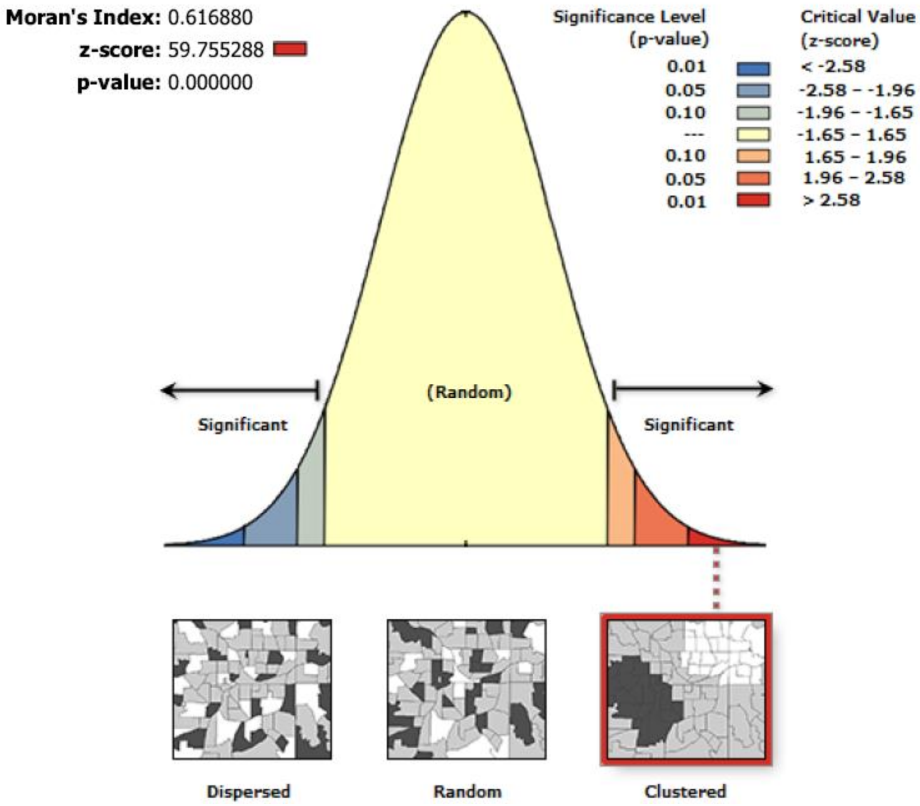

Figure 6. Shows the statistical analysis of the spatial distribution of the termite mounds, using Moran's, I global autocorrelation. The statistics returned a P value < 0.001 and Z value of 59.

4.3. The density distribution of the termite mounds.

The density distribution of termite mounds was estimated, using kernel density within the spatial statistics tool in ArcMap 10.5.1. The result is presented in Figure 7. The Kernel density presented below calculates the density of the termite mounds, per square kilometres. The red areas are highly populated with termite mounds of an average of 710 mounds per square kilometres, followed by the yellow areas which have an average density of 419 mounds per square kilometres, and the green areas with an average of 125 mounds per square kilometres. From the result, a general Hercynian trend could be observed within the spatial distribution of the mounds (F-F). The high density of the termite mounds is observed in the south-eastern portion of the research area (A), taking a north-northwest trend (B-B). The medium density of the mounds could be realised in most of the research area (C). The variation in the density of the termite mounds indicate the influence of spatial factor and also indicates the mound distribution is not random. Detailed discussion can be found in section 6.1.2.

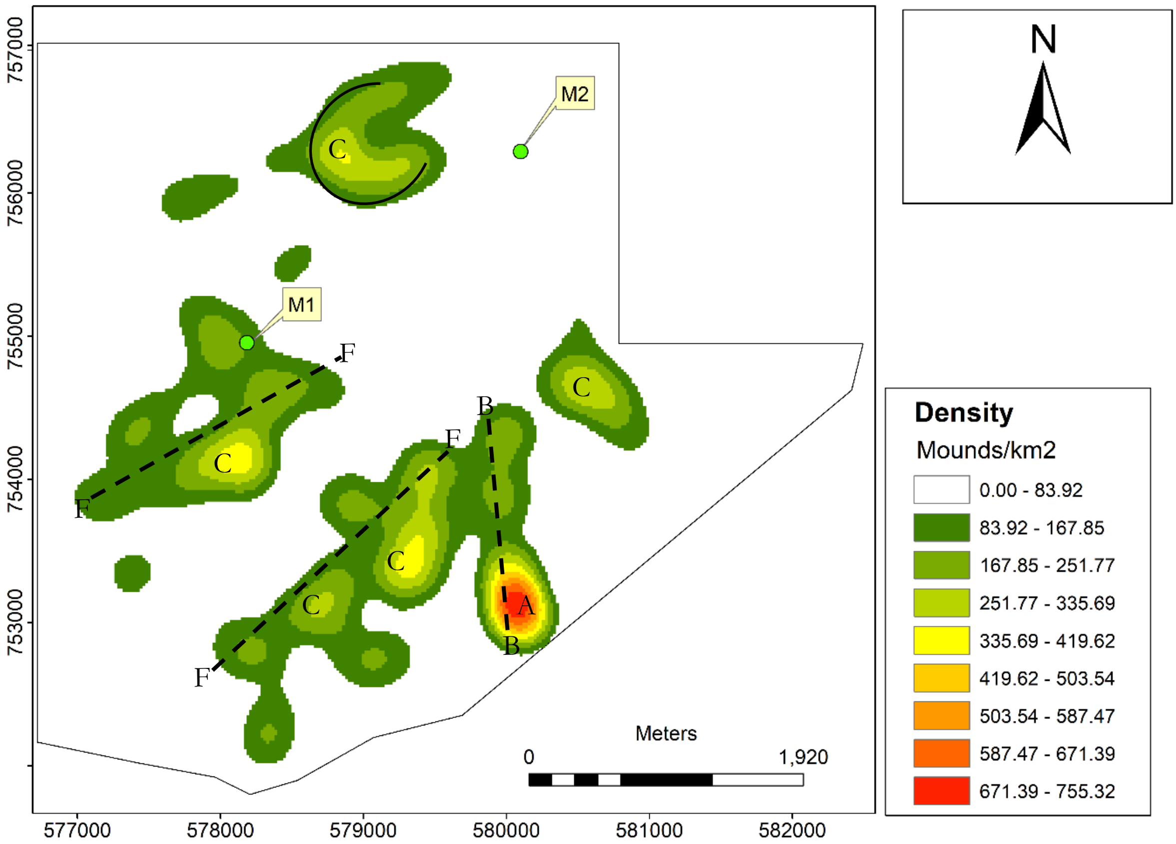

Figure 7. The figure shows the density distribution of the termite mounds in the research area.

4.4. Directional trend within the termite mound distribution.

The directional trend within the spatial distribution of the termite mound was determined, using standard deviational ellipsoidal trend analysis in ArcMap 10.5.1. The result is presented in Figure 8. The direction of the ellipsoid (elongation), gives a general trend of the orientations of the mounds within the research area. From the results, it could be seen that most of the ellipse around the distribution of the mound is elongated in the North-east, South-west direction (Hercynian). This general trend dominates from the West to the North-Western portion of the research area, and less within the south-eastern portion. Within the south-south-east to the western portion of the research area, a north-northwest trend is observed (A). The observed north-northwestern trend does not correlate with the general Hercynian trend observed. In the northern flanks of the research area, a semi-circular termite distribution is observed, encompassed by a circular directional trend. It is clear that the termites generally follow north-east, south-west trend, which is a significant trend within the birimian orogenic terrain of Ghana (Leube, Hirdes, Mauer, & Kesse, 1990).

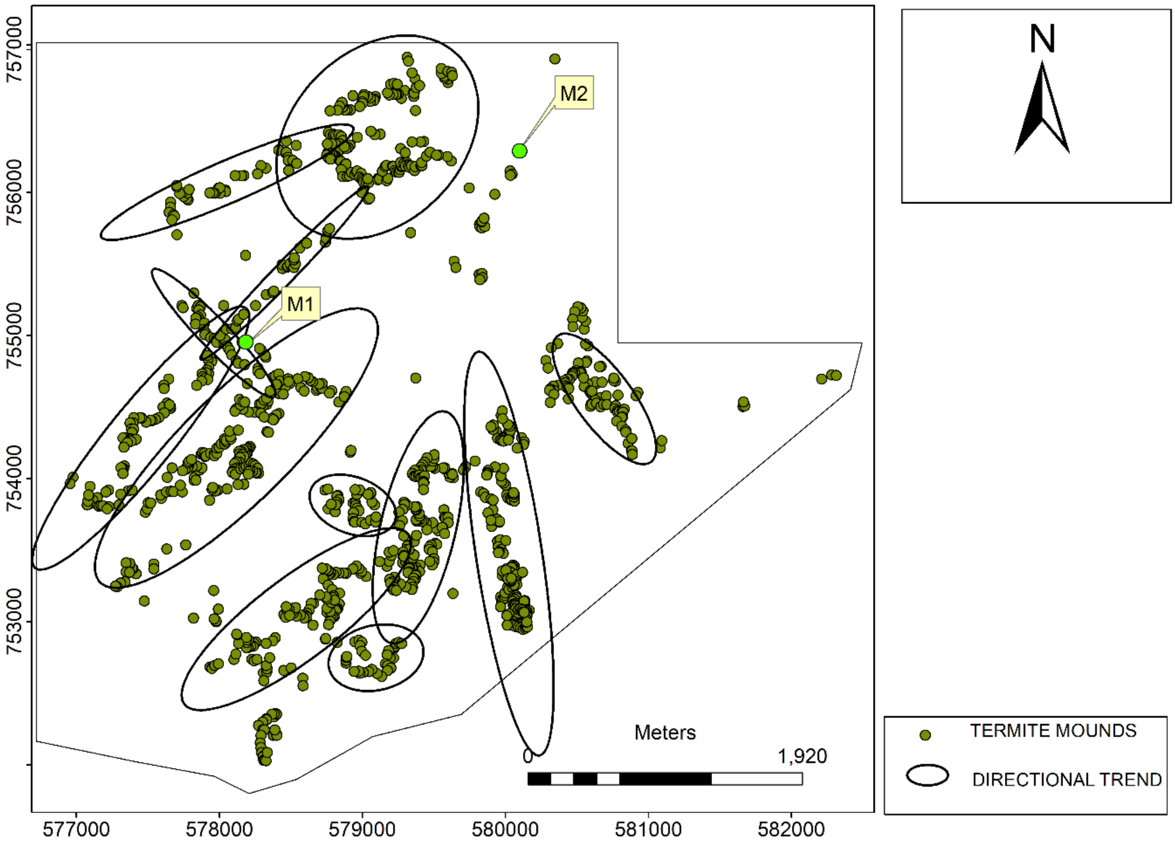

Figure 8. The directional orientation of the spatial distribution of the termite mounds. The direction of the ellipsoid gives a general trend of the orientation of the mounds.

4.5. Drainage pattern within the research area.

The surface drainage pattern of the research area was inferred from the SRTM data. The result is presented in Figure 9. From the results, the surface drainage shows a dendritic pattern within the research area. The surface drainage is seen to be flowing from the middle of the research area, mainly to the flanks of the research area.

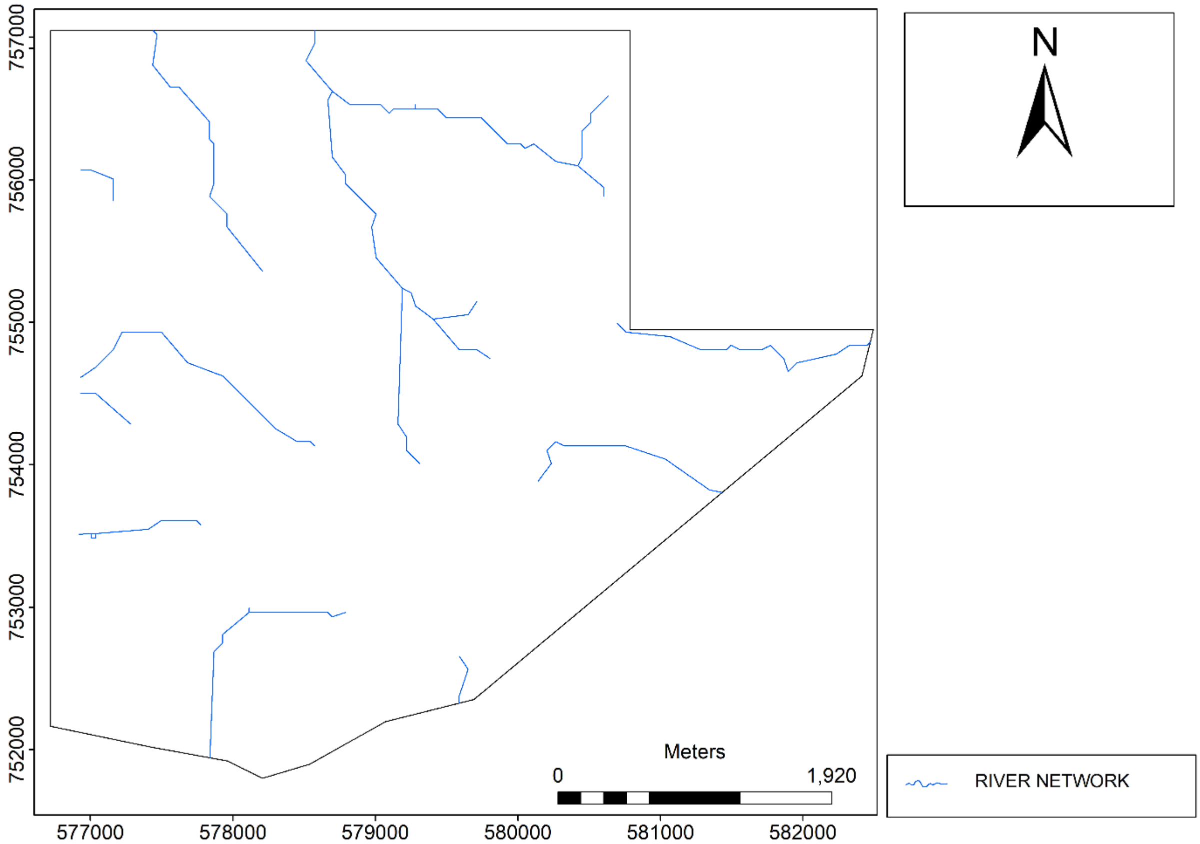

Figure 9. Surface drainage pattern within the research area.

4.6. The relationship between the directional trend of mound distribution and drainage.

The relationship between the inferred drainage pattern and the termite mound directional trend was accessed. The directional trend was superimposed on the drainage pattern. The relationship between the mound directional trend and the surface drainage was analysed to try to see if the directional trend of the termite mounds has any association with the surface drainage, and then try to rule out the possibility of the mound directional trend being influenced by the surface drainage. The result is presented in Figure 10 Below. From the result, it was clear that the mounds do not follow the drainage pattern within the research area. This indicates that the spatial distribution and directional trend of the mounds, does not follow the drainage pattern in the research area.

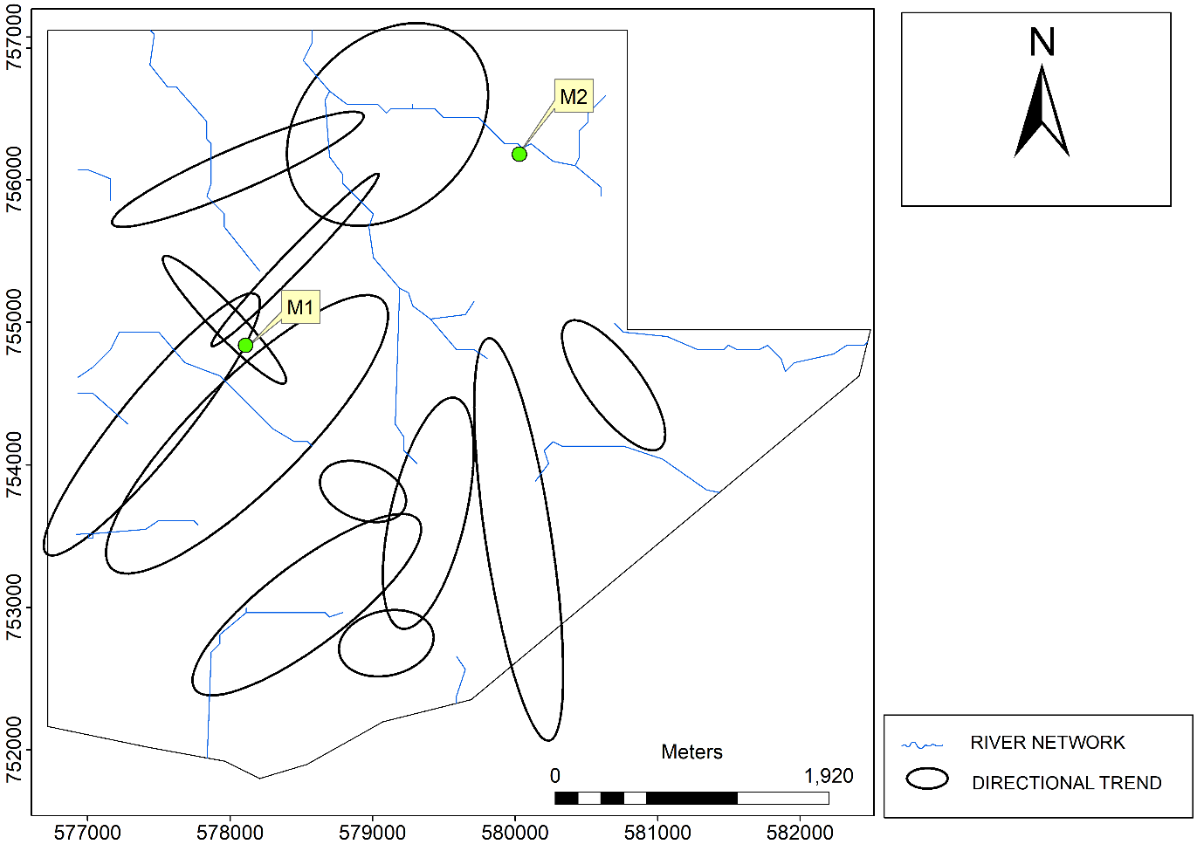

Figure 10. The directional trend of termite mounds superimposed on the SRTM interpreted surface drainage.

4.7. The relationship between the directional trend of termite mounds and aeromagnetic.

The relationship between the directional trend of the termite mounds and first vertical derivative (1VD) aeromagnetic of the research area was assessed. The directional trend of the termite mounds was superimposed on the aeromagnetic image and the aeromagnetic inferred faults. The 1VD aeromagnetic imagery enhances near surface features such as dykes, faults, and magnetic bodies (Oha et al., 2016). The aeromagnetic image is used here as a reference to compare with the directional trend of the distribution of the mounds. The result is presented in Figure 11. From the results, it could be observed that correlation exists between the trend of the termite mounds (Northeast, south-west) and areas of high magnetic anomalies (B). To the south-east, a north-northwest trend (V-V) is observed, correlating with the aeromagnetic inferred fault (A-A). Also, to the west of the research area, a northwestern trend (N-N) could be realised, which deviates from the north east south west trends in the research area. This cut across different magnetic bodies (C). The relationship between the mound and the high magnetic anomalies indicates the termites are generally following zones of high magnetic anomalies. This is however further explained in section 6.1.3.

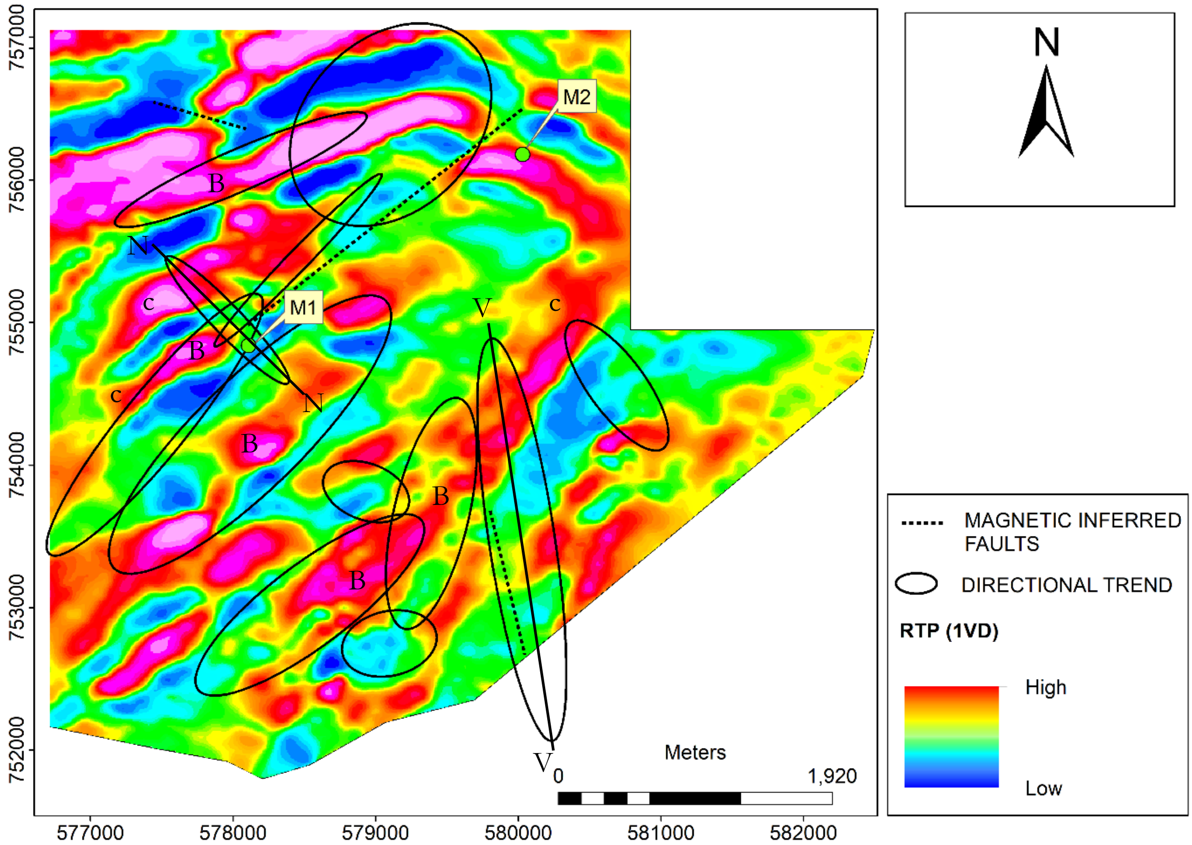

Figure 11. The directional trend of the termite mounds distribution, superimposed on reduced to pole first vertical derivative (RTP-1VD) aeromagnetic data. The aeromagnetic inferred faults were manually inferred from the RTP-1VD.

4.8. The relationship between the directional trend of termite mounds and chargeability.

The directional trend of the termite mounds was superimposed on the chargeability image of the research area. The result is presented in Figure 12. The colours in the figure represent chargeability of the subsurface; "sgi beat" and red represent high chargeability, whiles blue, represents low chargeability respectively. From the results, a general correlation between the termite mound trend (NE-SW) and high chargeability areas could be observed (A). To the north of the research area, a highly positive correlation could be observed between the mound distribution and a semi-circular high chargeable zone (C).

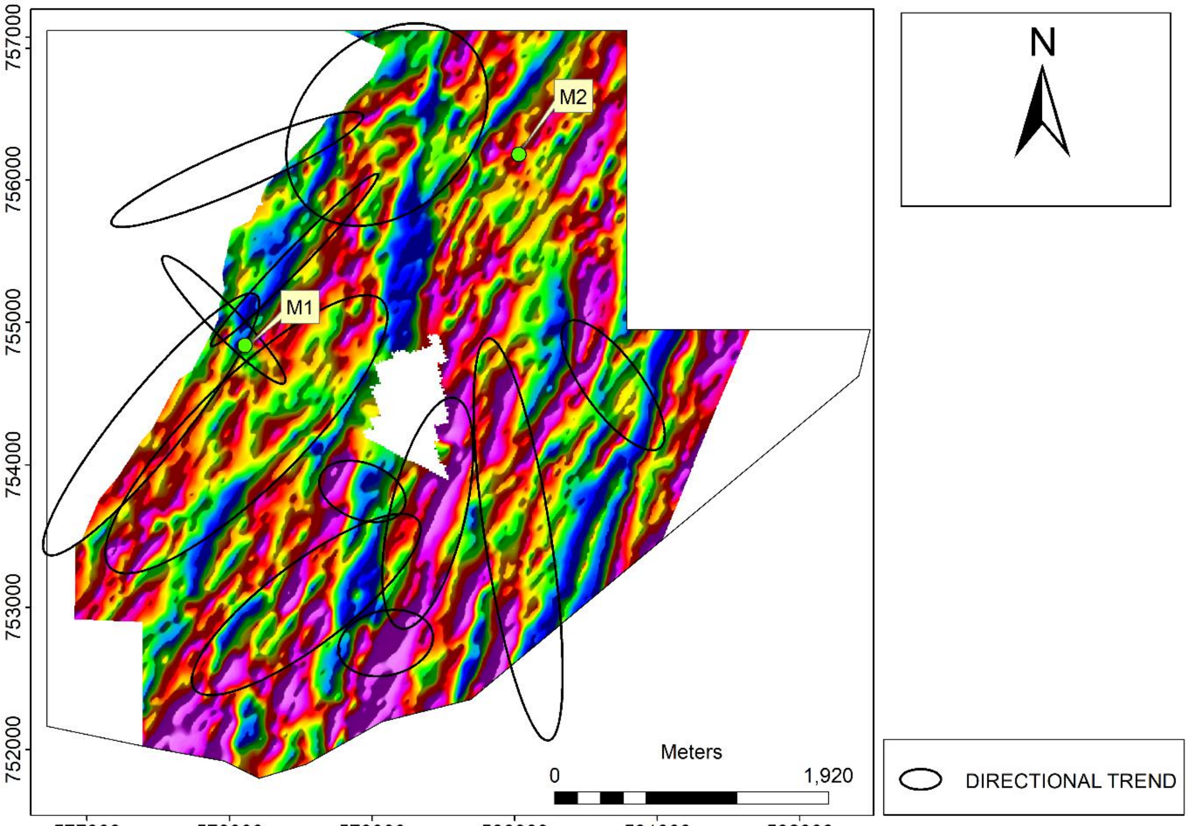

Figure 12: The directional trend of termite mounds, superimposed on the chargeability of the subsurface. “Sgi beat” to red represents high chargeability; whiles “blue” represents low chargeability.

4.9. The relationship between the directional trend of termite mounds and major faults.

The relationship between the directional trend of termite mounds and major faults within the research area was assessed. The result is presented in Figure 13. From the results, the termite mounds generally trend northeast south-west, which is not different from the major fault trends in the research area(Consulting, 2013). It could be realised that the termite mounds have a very good association with the major fault trends, except some few termite mounds that trend almost at right angle to the major faults in the research area. The association of the termites with the major fault trend indicates the termites may be following the fault structures within the research area, possibly in search of weathered clay products and moisture. This is further discussed in section 6.1.5

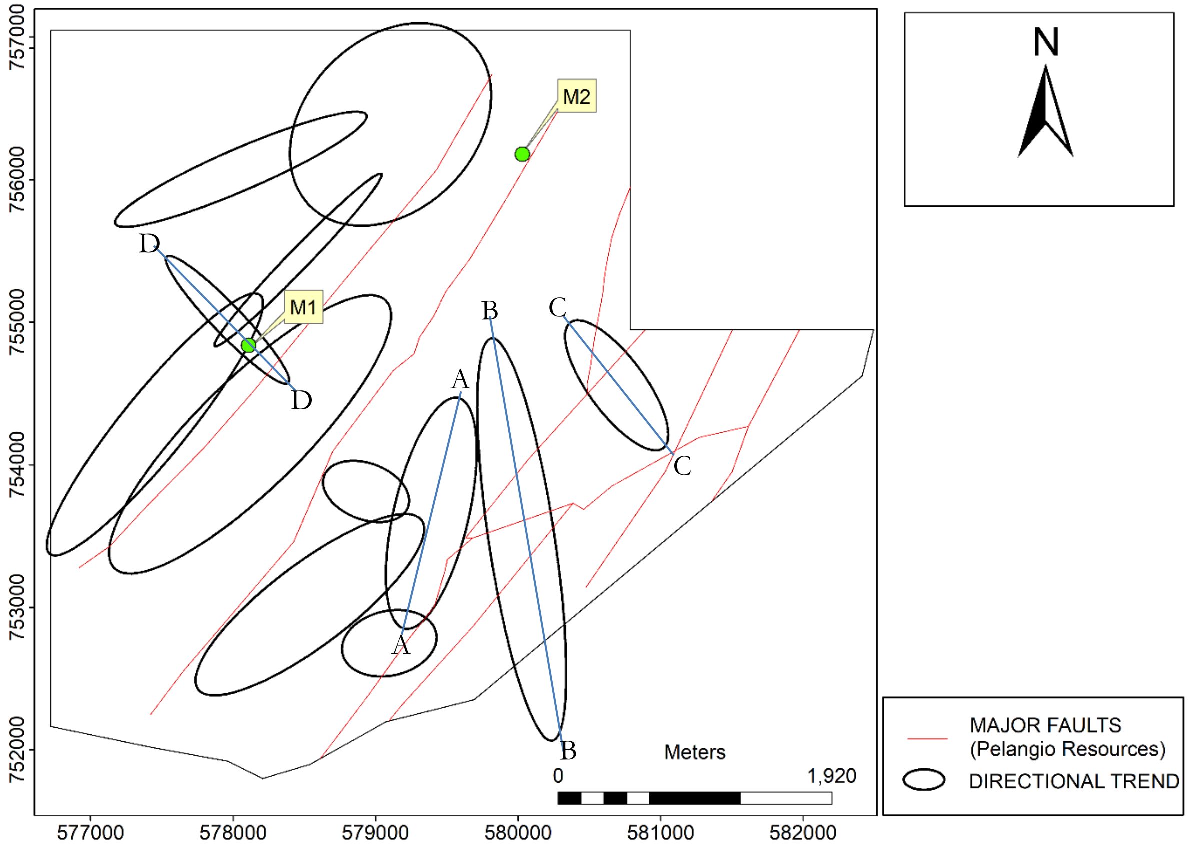

Figure 13. The directional trend of termite mounds superimposed on published major faults in the research area. The major faults map, provided by Pelangio Resources (Pelangio Resources, 2015).

5. MINERALOGICAL AND GEOCHEMICAL RESULTS OF THE TWO SELECTED TERMITE MOUNDS.

5.1. Mineralogy of termite mound 1 and 2.

X-ray powder diffraction (XRD) analysis was performed on the passing fraction of the termite mounds and the subsurface samples. XRD is a rapid analytical technique used for phase identification of crystalline material. The XRD was used to determine the mineral composition of the termite mound and the subsurface samples. Results of selected samples from termite mounds one (M1) and the subsurface is presented in Figure 14, while that of termite mound two (M2) and the subsurface is presented in Figure 15. From the figures, the presence of clay mineral (kaolinite) at 2θ 11.6°, quartz at 2θ 26.5° both within the mound and the subsurface for the different mounds could be realised. The quartz peak is seen to have high intensity, which influences the intensity of the XRD inferred kaolinite peaks, within both the subsurface and the mound see Figure 14. The influence of the quartz peak is seen dominated between 2(θ) 26.1° and 27.3° both on Figure 14 and Figure 15. This effect is present in all the analysed samples both from the termite mounds and their immediate subsurface, see Appendix 1 to 1.3. Upon careful analysis, the intensity of the quartz diffractogram is seen to subdue the intensity of the kaolinite diffractograms peaks between 2(θ) 19.8° and 2 (θ) 25.7°, which is relevant to determine the crystallinity of kaolinite (Artioli et al., 1995).

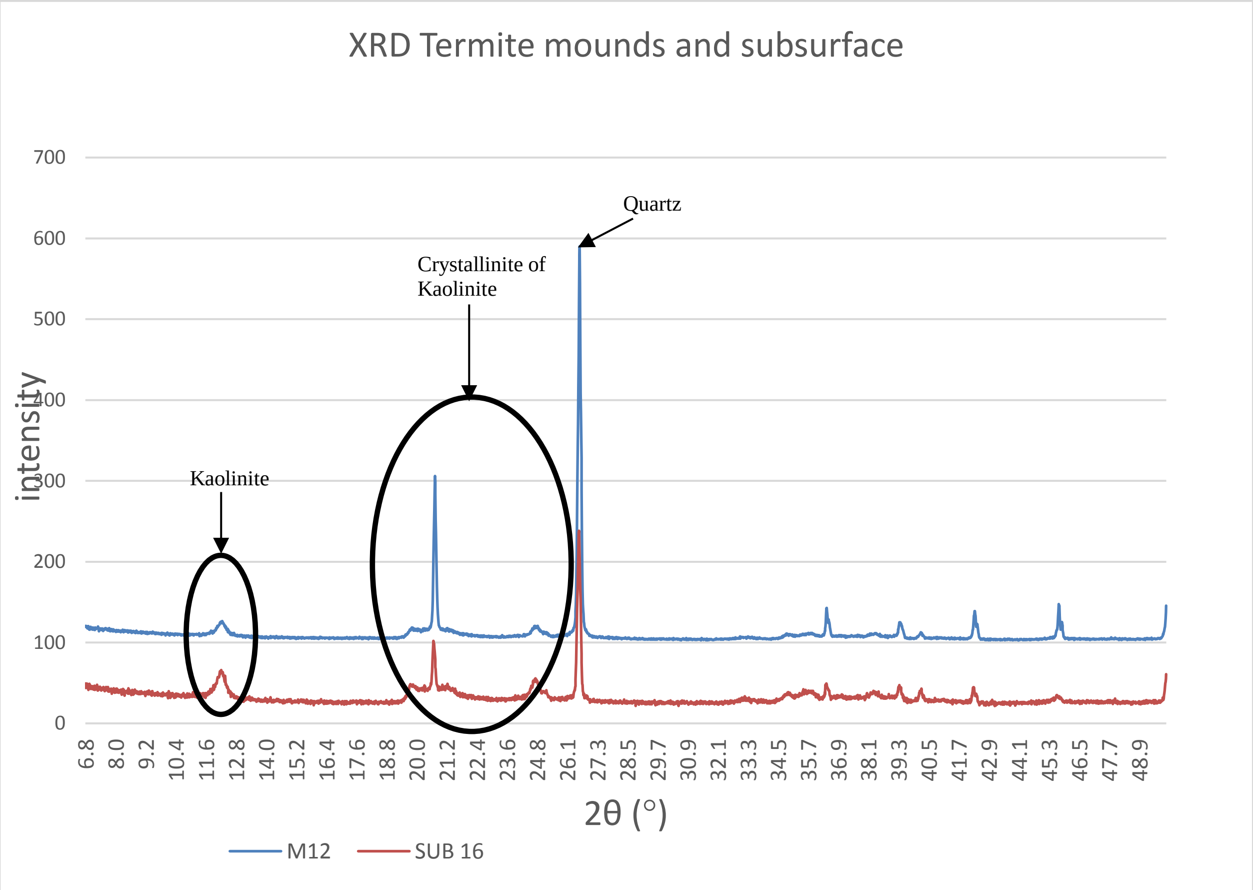

Figure 14. XRD results of selected termite mound, and subsurface. Sample (M12 and SUB 16), from termite mound 1. M12 is from the termite mound, SUB16 from the subsurface. The result has been offset for clarity.

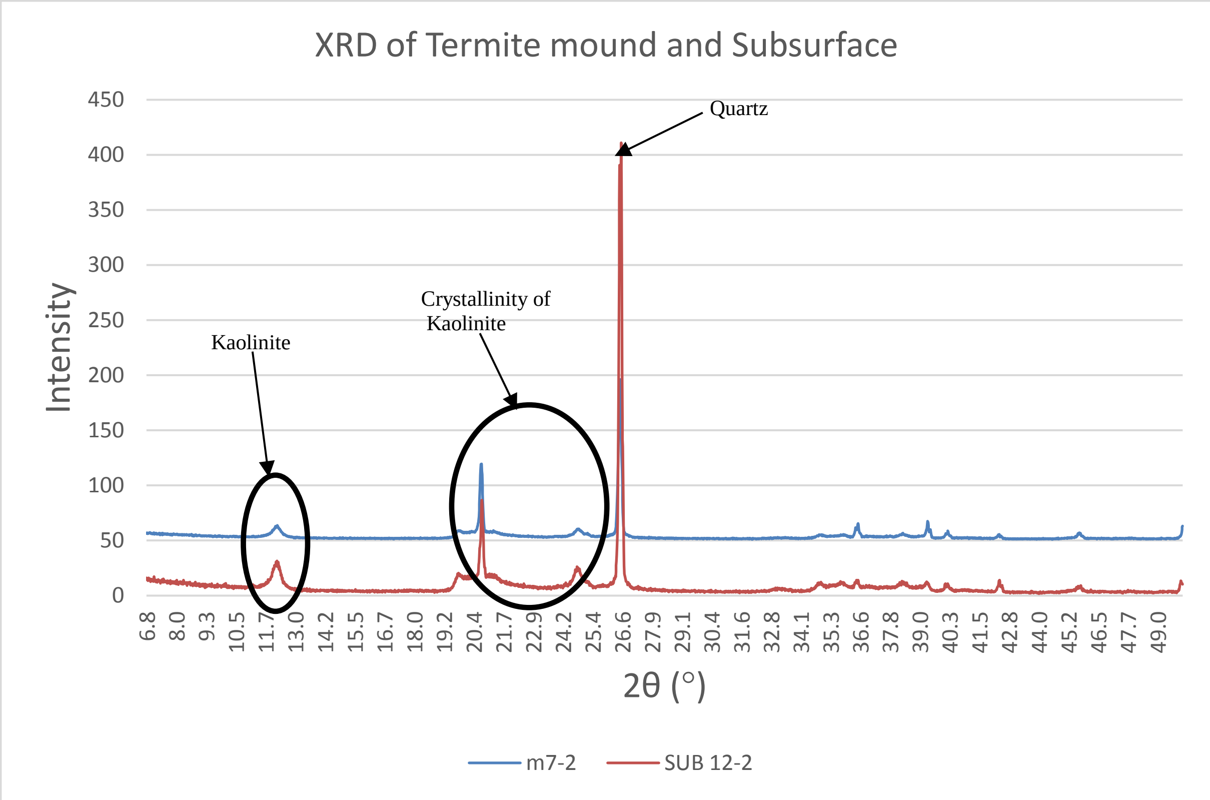

Figure 15. XRD results of selected termite mound, and subsurface. Sample (M7-2 and SUB12-2), from termite mound 2. M7-2 is from the termite mound; SUB 12-2 is from the subsurface. The result has been offset for clarity.

5.2. Crystallinity of kaolinite from termite mounds 1 and 2.

The crystallinity of kaolinite from the two termite mounds was determined by separating the clay mineral from the two (2) selected mound sample, since the presence of quartz influenced the intensity of the diffractogram peaks, as can be seen in Figure 14 and Figure 15 above. The XRD analysis was performed on the resulting clay proportion and visually interpreted by analysing the diffractogram of the selected samples from the two termite mounds at 2(θ), from 19.8° to 25.7°, as suggested by Artioli et al., (1995).This was then compared to the diffractogram of two natural kaolinite samples: disordered and ordered kaolinites see Figure 17. Here, the presence or absence of diffractogram peaks (intensities), between 2(θ) 19.8° and 2(θ) 25.7°, which suggests ordered or disordered kaolinite respectively was used. Finally, the result is supported by the crystallinity index calculated from the XRD diffractogram (M12=75, M7-2= 78). The result is presented in Figure 16 below. From the results, it is clear that there is no major difference between the diffractograms from the two termite mounds, which suggest the termites are primarily transporting similar materials from the subsurface. The peaks of the clay mineral (kaolinite) at 2(θ) 20.139° (A), 2(θ) 21.062° (B), and 2(θ) 21.581° (C), Figure 16, shows enough intensities. This is no different from the peaks observed from the crystalline reference kaolinite sample (B), see Figure 17. However, there are two missing peaks at 2(θ) 23.197° (E) and 2(θ) 23.774° (F), which suggest that the clay mineral kaolinite has undergone some form of modification, probably due to surface regolith processes, or transportation from the subsurface to the surface.

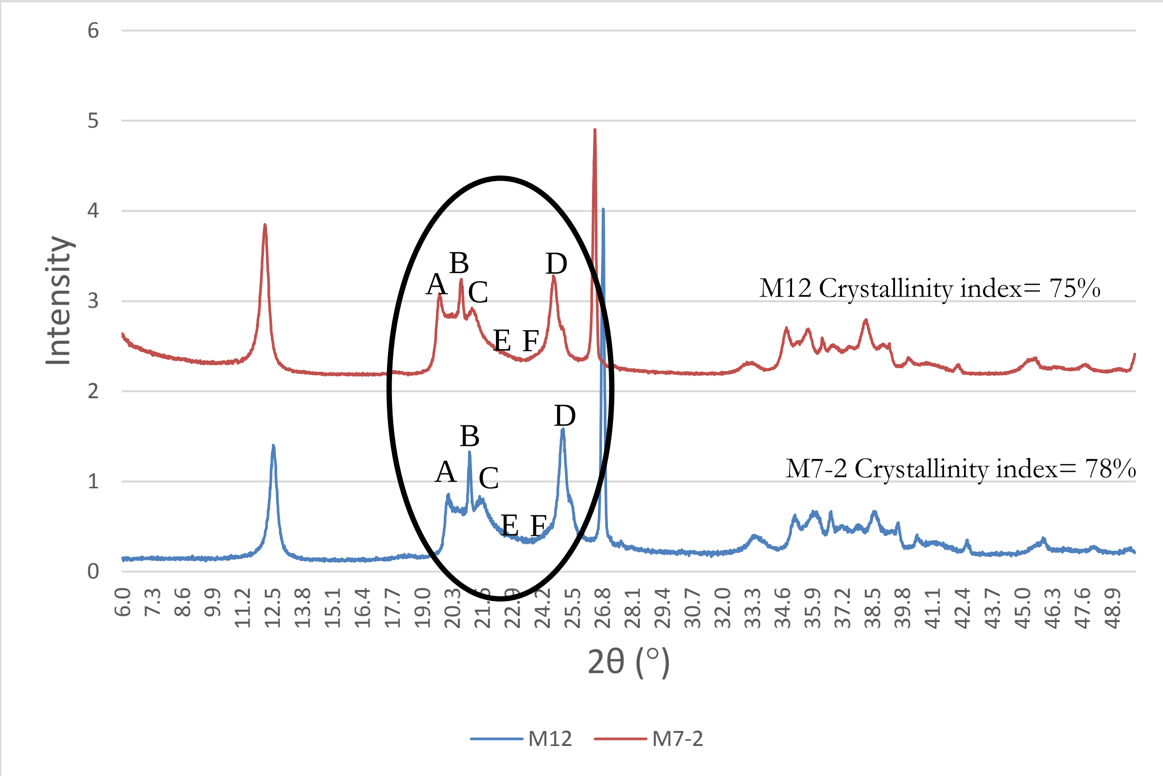

Figure 16. XRD results of M12 (mound 1) and M7-2 (mound 2), after sedimentation. The result shows the crystallinity of kaolinite around 19.8°, and 21.7°, 2(θ).

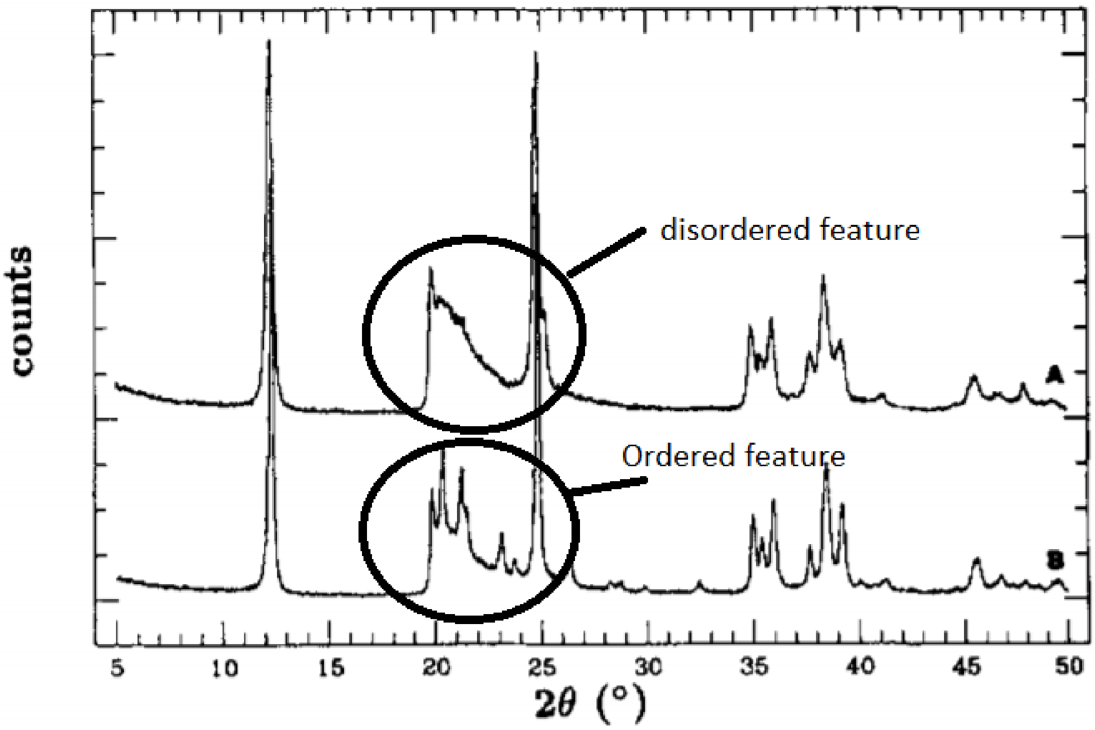

Figure 17. Modified after Artioli et al., (1995). X-ray powder diffraction patterns for two natural reference kaolinite samples: (A) poorly crystallised kaolinite KGA-2 from Warren County, Georgia, United States: (B) well-crystalline kaolinite from Nuraghe Mandras sas Ebbas, Sardina, Italy. The profile has been shifted relative to the vertical axis, and the vertical units refer to profile B.

5.3. Mineralogy of termite mound 1 and 2 using (VNIR-SWIR-Spectroscopy).

Mineralogical analysis of selected termite mound and the subsurface was performed using VNIR-SWIR spectroscopy. The result is presented in Appendix 1.4 and 1.5. The spectra show absorption features for goethite at 0.5 um, hematite at 0.9 um, kaolinite centred at 2.16 and 2.2 um, both in the termite mound and the subsurface. The presence of the kaolinite confirms the primary mineral identified in the XRD analysis (kaolinite). It could be seen that the minerals identified in the termite mound are not different from its subsurface. This confirms the fact that the termites sample the subsurface to build their mounds (Ali, Ahmed, Sheridan, & French, 2016).

5.4. Crystallinity of kaolinite from termite mound 1 and 2 (VNIR-SWIR- Spectroscopy).

Kaolinite is found in most weathered regolith and lateritic environments. The mineral is also seen as a typical hydrothermal alteration product in many types of deposits. The crystallinity of kaolinite could be used to infer its provenance. Highly crystalline kaolinite could be related to residual, whiles poorly crystalline kaolinite could be related to surface regolith processes (transported sediments) (Cudahy, 1997). The crystallinity of kaolinite was determined on the selected termite mound samples (M12 and M7-2). The result is presented in Figure 18. The spectra have been zoomed from 1.0 to 2.5 for clarity of the absorption feature. The absorption feature for kaolinite at 2.2086 was used, since well-crystallised kaolinite, is expected to have a sharp absorption at 2.2086 ± 0.0003 μm (Clark, 1999). Also, the spectra from the mound samples were compared to standard crystalline spectra from the USGS spectral library. From the results, the kaolinite spectra from the mound is seen to have an asymmetric doublet structure in the 2.2 and the 1.4 micrometres (um) region, compared to the crystalline kaolinite from the USGS library. At 2.1650 um region, the minima shoulder of the kaolinite doublet, from the termite mounds is softened as can be seen in Figure 18. This indicates decreasing order in the crystal structure (Spectral international INC, 2018). This further indicates that the clay mineral (kaolinite) in the termite mound could have been affected by surface regolith processes. Hence its provenance could be related to a semi-residual environment, where mineralisation could be partly related to the subsurface. This is inferred from the structure of kaolinite since it is not entirely disordered.

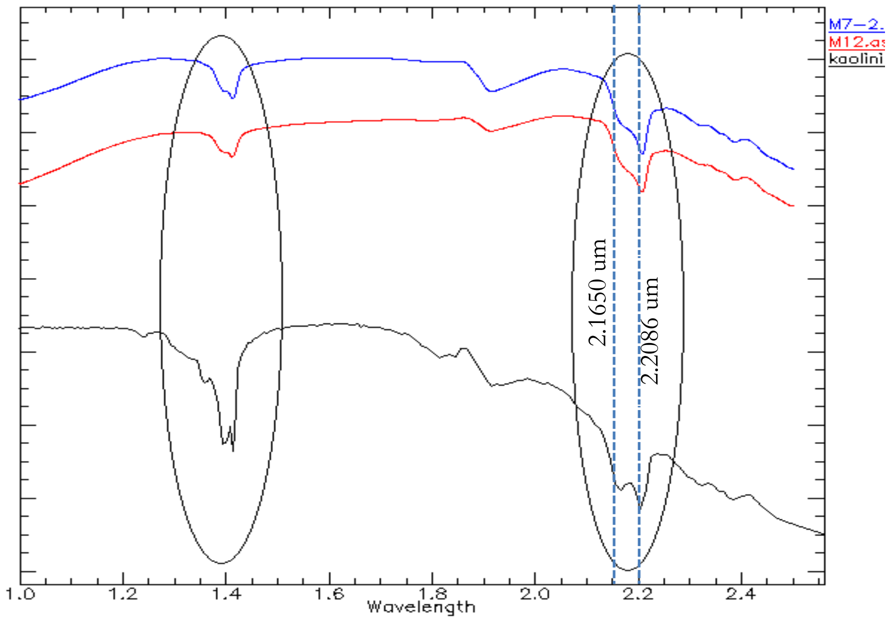

Figure 18. M12 and M7-2 VNIR-SWIR spectra of termite mound samples from termite mound 1 and 2, compared to a standard, crystalline kaolinite spectrum from the USGS spectra library. The spectra have been expanded from 1.0 um to 2.5 um and offset for clarity of the kaolinite absorption features. The black spectra is the standard USGS crystalline spectra of kaolinite, while the red and blue spectra represent the spectra from termite mound 1 and 2 respectively.

5.5. Geochemistry of termite mounds 1 and 2.

The chemistry of the two termite mound samples was determined using ICP-OES elemental analysis. The result for the major and trace elements including gold (Au) is presented in Appendix 1.6. The calibration line for Au (ICP-OES) was realised to be faulty. This might overestimate the concentration of Au; hence, resulting in higher concentration of Au within both mounds and the subsurface. This effect was considered in the interpretation of the Au results in this research. Selected major elements in percentage from "M1" and "M2" is presented in Table 1 and 2 respectively. The elemental concentrations are based on two termite mounds and their immediate subsurface, from the different geophysical environment. Descriptive statistics have been performed on selected major elements in percentage (Table 3), and major and trace elements in mg/kg (Table 4). From Table 3, considering the standard deviation of the elements, compared to their means, it could be seen that the standard deviation is low compared to the mean, which suggests that the concentration of the elements is close to their mean concentration. This is however not the same for Table 4. The difference could be attributed to the fact that in table 1 only major elements were selected, whiles in table 2, both the major and trace elements were selected for the statistical analysis.

Table 1. ICP-OES results of termite mound 1 and the immediate subsurface.

Sample Id	Al (%)	Ca (%)	**Mg (%)**	K (ppm)	Mg/Al	K/Al
			Mound 1			
M2	8.24×10^{0}	5.58×10^{-2}	8.02×10^{-2}	2.13×10^{-2}	9.74×10^{-3}	2.58×10^{-3}
M8	7.79×10^{0}	4.51×10^{-2}	8.25×10^{-2}	3.75×10^{-2}	1.06×10^{-2}	4.81×10^{-3}
M12	7.74×10^{0}	4.07×10^{-2}	8.10×10^{-2}	4.00×10^{-4}	1.05×10^{-2}	5.20×10^{-5}
M16	7.28×10^{0}	4.27×10^{-2}	7.68×10^{-2}	1.00×10^{-5}	1.05×10^{-2}	1.00×10^{-6}
M18	7.68×10^{0}	4.25×10^{-2}	7.87×10^{-2}	1.01×10^{-5}	1.02×10^{-2}	1.01×10^{-6}
M20	7.82×10^{0}	4.23×10^{-2}	8.15×10^{-2}	1.02×10^{-5}	1.04×10^{-2}	1.02×10^{-6}
M22	7.42×10^{0}	4.32×10^{-2}	7.91×10^{-2}	1.03×10^{-5}	1.07×10^{-2}	1.03×10^{-6}
M24	7.91×10^{0}	5.08×10^{-2}	8.43×10^{-2}	1.04×10^{-5}	1.07×10^{-2}	1.04×10^{-6}
M28	7.87×10^{0}	4.86×10^{-2}	8.41×10^{-2}	1.05×10^{-5}	1.07×10^{-2}	1.05×10^{-6}
M32	7.84×10^{0}	4.69×10^{-2}	7.94×10^{-2}	1.06×10^{-5}	1.01×10^{-2}	1.06×10^{-6}
			Subsurface 1			
Sub1	7.60×10^{0}	2.95×10^{-2}	7.30×10^{-2}	1.83×10^{-1}	9.61×10^{-3}	2.41×10^{-2}
sub3	8.03×10^{0}	3.48×10^{-2}	7.84×10^{-2}	2.21×10^{-1}	9.76×10^{-3}	2.75×10^{-2}
sub 4	4.01×10^{0}	2.82×10^{-2}	4.20×10^{-2}	2.94×10^{-1}	1.05×10^{-2}	7.34×10^{-2}
sub6	9.44×10^{0}	2.92×10^{-2}	8.41×10^{-2}	2.42×10^{-1}	8.91×10^{-3}	2.56×10^{-2}
sub8	1.04×10^{1}	2.71×10^{-2}	9.22×10^{-2}	2.75×10^{-1}	8.88×10^{-3}	2.65×10^{-2}
sub9	9.51×10^{0}	3.44×10^{-2}	8.86×10^{-2}	2.08×10^{-1}	9.31×10^{-3}	2.18×10^{-2}
sub11	1.07×10^{1}	2.58×10^{-2}	9.73×10^{-2}	1.61×10^{-1}	9.05×10^{-3}	1.50×10^{-2}
sub12	1.08×10^{1}	3.05×10^{-2}	9.69×10^{-2}	1.50×10^{-1}	9.01×10^{-3}	1.39×10^{-2}
sub14	1.04×10^{1}	2.91×10^{-2}	9.11×10^{-2}	7.62×10^{-2}	8.72×10^{-3}	7.30×10^{-3}
s16(15)	1.09×10^{1}	2.91×10^{-2}	9.59×10^{-2}	7.65×10^{-2}	8.82×10^{-3}	7.04×10^{-3}
s17(13)	1.08×10^{1}	3.03×10^{-2}	8.77×10^{-2}	3.66×10^{-2}	8.14×10^{-3}	3.39×10^{-3}
SUB 20	1.06×10^{1}	3.02×10^{-2}	9.59×10^{-2}	2.60×10^{-2}	9.01×10^{-3}	2.45×10^{-3}

Table 2. ICP-OES results of termite mound 2 and the immediate subsurface.

Sample Id	Al (%)	Ca (%)	Mg (%)	K (%)	Mg/Al	K/Al
	Mound 2					
M1-2	7.48×10^{0}	3.22×10^{-2}	9.07×10^{-2}	1.00×10^{-5}	1.21×10^{-2}	1.00×10^{-6}
M3-2	7.27×10^{0}	3.21×10^{-2}	8.78×10^{-2}	1.00×10^{-5}	1.21×10^{-2}	1.00×10^{-6}
M5-2	7.14×10^{0}	4.18×10^{-2}	9.73×10^{-2}	1.00×10^{-5}	1.36×10^{-2}	1.00×10^{-6}
M7-2	7.21×10^{0}	3.61×10^{-2}	8.64×10^{-2}	1.00×10^{-5}	1.20×10^{-2}	1.00×10^{-6}
M10-2	6.10×10^{0}	8.55×10^{-2}	9.01×10^{-2}	1.00×10^{-5}	1.48×10^{-2}	2.00×10^{-6}
M12-2	6.44×10^{0}	7.37×10^{-2}	9.13×10^{-2}	1.00×10^{-5}	1.42×10^{-2}	2.00×10^{-6}
M15-2	7.30×10^{0}	2.45×10^{-2}	8.25×10^{-2}	1.00×10^{-5}	1.13×10^{-2}	1.00×10^{-6}
M17-2	7.53×10^{0}	2.96×10^{-2}	8.75×10^{-2}	1.00×10^{-5}	1.16×10^{-2}	1.00×10^{-6}
M19-2	7.76×10^{0}	2.42×10^{-2}	9.00×10^{-2}	1.00×10^{-5}	1.16×10^{-2}	1.00×10^{-6}
M20-2	6.84×10^{0}	8.24×10^{-2}	8.24×10^{-2}	1.00×10^{-5}	1.21×10^{-2}	1.00×10^{-6}
	Subsurface 2					
S1-2	6.97×10^{0}	6.85×10^{-2}	9.49×10^{-2}	1.00×10^{-5}	1.36×10^{-2}	1.00×10^{-6}
SUB2-2	7.46×10^{0}	3.39×10^{-2}	8.67×10^{-2}	1.00×10^{-5}	1.16×10^{-2}	1.00×10^{-6}
SUB4-2	7.70×10^{0}	3.10×10^{-2}	8.88×10^{-2}	1.00×10^{-5}	1.15×10^{-2}	1.00×10^{-6}
S7-2	8.00×10^{0}	2.19×10^{-2}	8.38×10^{-2}	1.00×10^{-5}	1.05×10^{-2}	1.00×10^{-6}
SUB9-2	1.16×10^{1}	1.78×10^{-2}	1.02×10^{-2}	1.00×10^{-5}	8.74×10^{-3}	1.00×10^{-6}
SUB10-2	1.06×10^{1}	2.90×10^{-2}	9.09×10^{-2}	1.00×10^{-5}	8.58×10^{-3}	1.00×10^{-6}
SUB12-2	1.01×10^{1}	2.10×10^{-2}	9.22×10^{-2}	1.00×10^{-5}	9.09×10^{-3}	1.00×10^{-6}
SUB16-2	1.13×10^{1}	2.50×10^{-2}	8.34×10^{-2}	1.00×10^{-5}	7.39×10^{-3}	1.00×10^{-6}
S17-2	1.04×10^{1}	2.80×10^{-2}	9.42×10^{-2}	1.00×10^{-5}	9.03×10^{-3}	1.00×10^{-6}

Table 3. Statistics of selected major elements in %.

	N	Minimum	Maximum	Mean	Std. Deviation
Al (%)	41	4.01	11.63	8.44	1.71
Fe (%)	41	1.90	7.23	3.94	1.03
Ca (%)	41	0.02	0.09	0.04	0.01
Mg (%)	41	0.04	0.10	0.09	0.01
N (listwise)	41				
Mg (%)	41	0.04	0.10	0.01	0.00
Valid N (listwise)	41				

Table 4. Statistics of major and trace elements in ppm.

	N	Minimum	Maximum	Mean	Std. Deviation
Mg (ppm)	41	419.70	1016.44	861.70	96.53
K (ppm)	41	0.01	2943.02	489.71	882.68
Ca (ppm)	41	177.52	855.28	365.83	142.38
Zn (ppm)	41	16.56	49.27	33.72	6.49
In (ppm)	41	17.21	47.35	32.86	5.55
Ca (ppm)	41	181.99	876.81	374.81	146.11
Fe (ppm)	41	19049.75	72309.88	39407.38	10280.59
Al (ppm)	41	40072.15	116263.26	84411.30	17052.36
Au (ppm)	41	1.41	156.58	107.19	43.48
N (listwise)	41				

5.6. Variation of the major elements and Gold (Au) within termite mound 1 and 2 and their subsurface.

The variation of the major elements (Mg, Al, and K), used in classifying the subsurface, in Figure 30 and 31, was accessed within the termite mounds and their immediate subsurface. The result is presented in Figure 19 to 24 and further discussed in section 6.2.2.

5.6.1. Variation of selected major elements and Gold within termite mound 1 and 2 and the immediate subsurface.

Termite mound 1

Termite mound 2

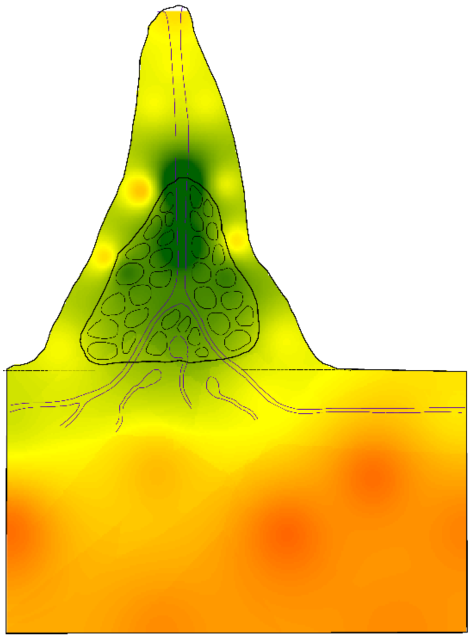

Figure 19. Variation of Mg within mound 1

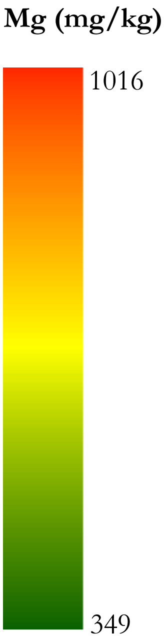

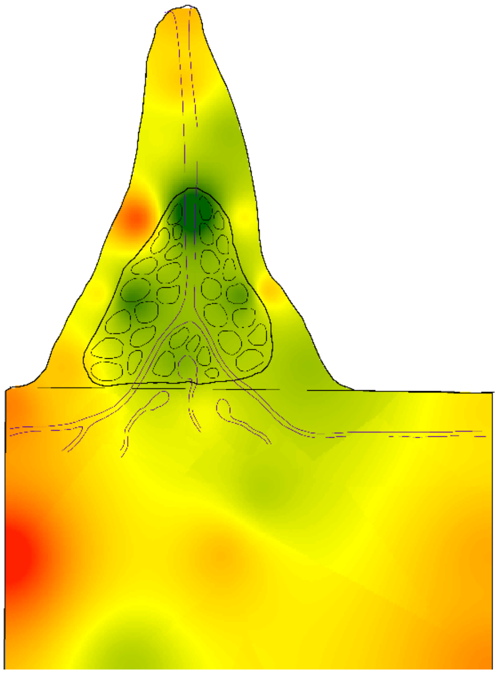

Figure 20. Variation of Mg within mound 2

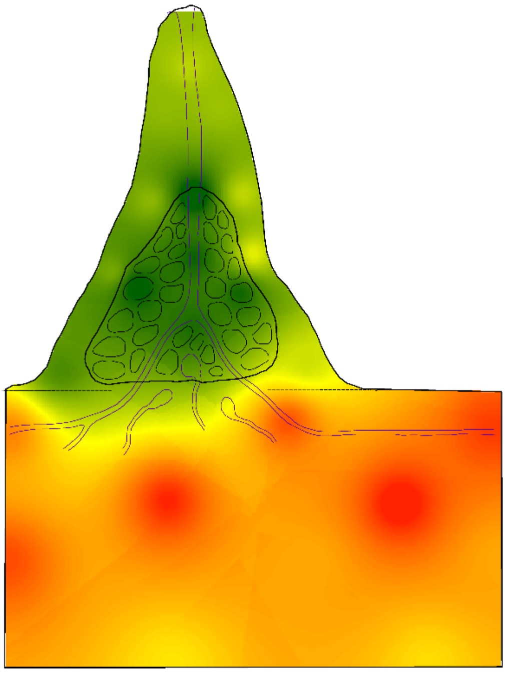

Figure 21. Variation of k within mound 1

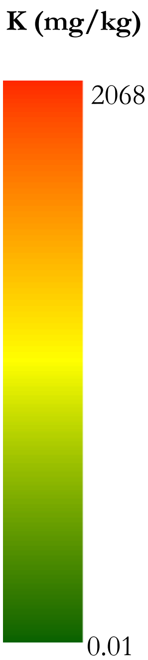

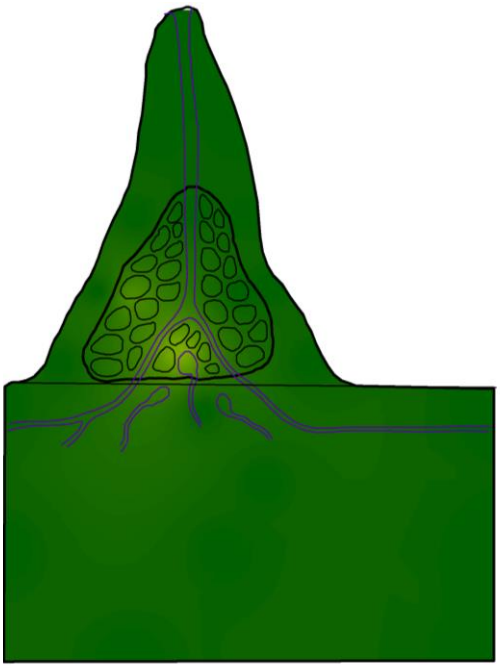

Figure 22. Variation of k within mound 2

Termite mound 1

Termite mound 2

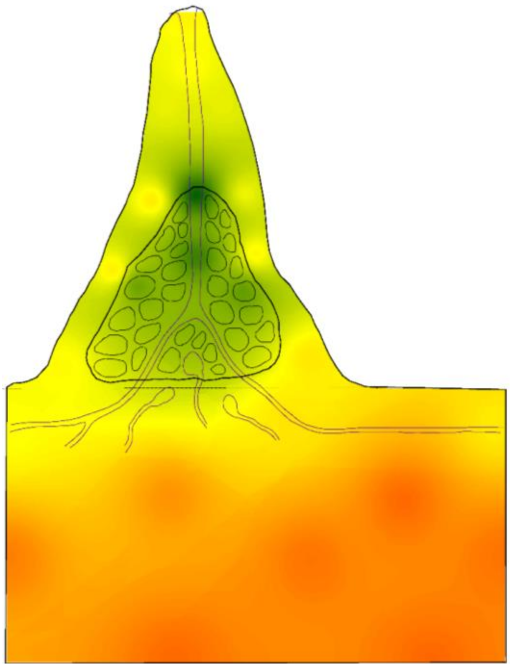

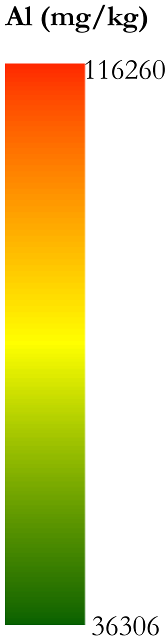

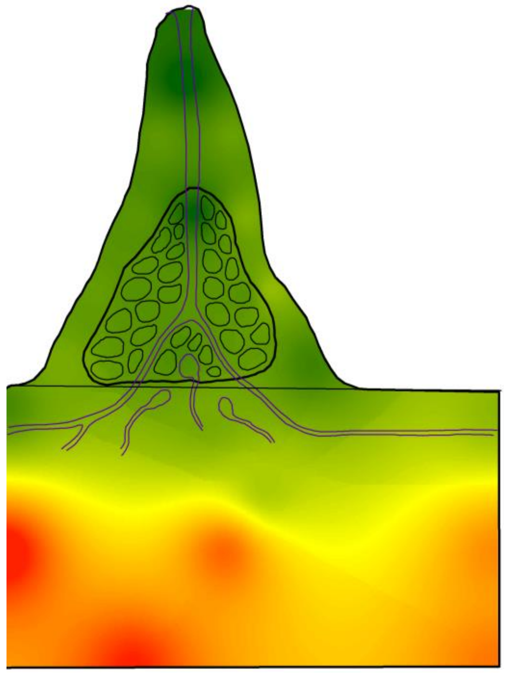

Figure 23. Variation of Al within mound 1.

Figure 24. Variation of Al within mound 2.

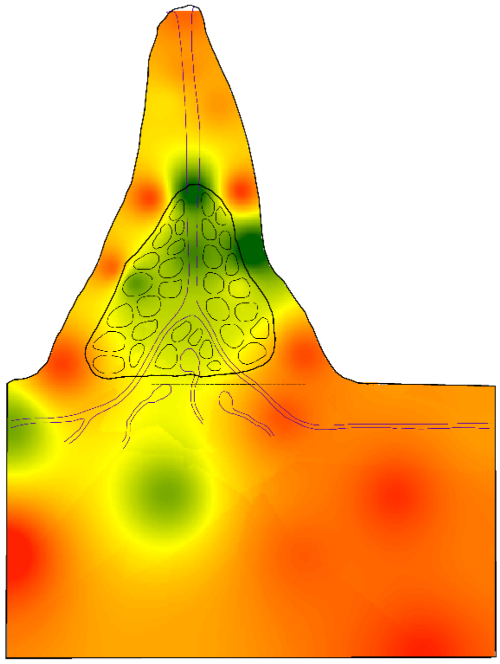

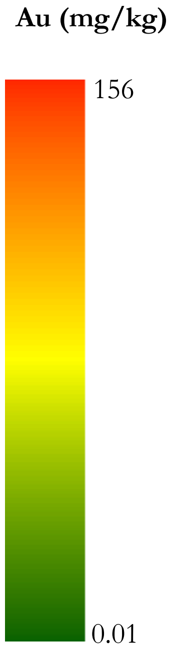

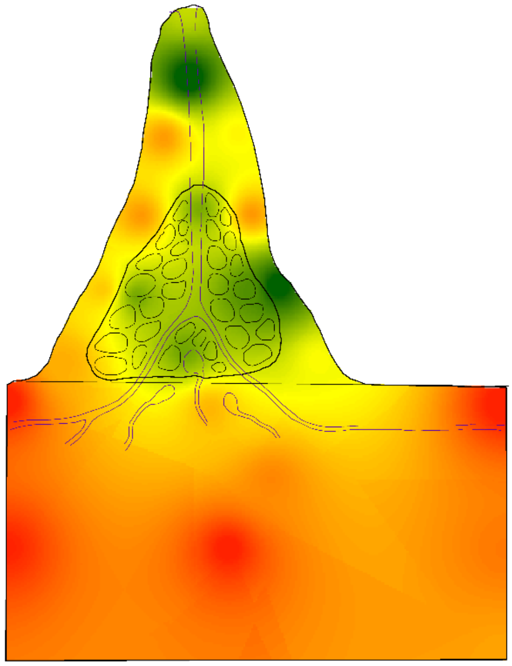

Figure 25. Variation of Au within mound 1.

Figure 26. Variation of Au within mound 2.

6. DISCUSSION.

6.1. Spatial analysis of termite mounds.

6.1.1. Spatial distribution of termite mounds.

The result of the statistical analysis, returned a Moran's Index of 0.62, with a significance of 0.01(P-value), a Z-score of 59.75, and a critical value greater than 2.5. The Moran's Index of 0.62 indicates that the termite mounds appear to have some degree of clustering, within the distribution. The P-value indicates that the clustering within the mound spatial distribution is statistically highly significant at less than 0.01. The Z-score of 59.75 indicates that the spatial distribution of the mound is not as a result of random chance (Getis & Ord, 1992). Hence the null hypothesis stating that the distribution of the termite mounds is as a result of random chance is rejected. Although the statistical result suggests non-random distribution, it is worth noting that, the rejection of the null hypothesis, does not mean total acceptance of the alternate hypothesis; which states that, the spatial distribution of the mounds is not by random chance. Froom the spatial autocorrelation, the clustering within the mounds, suggests, there could be some spatial factor influencing the mound distribution. It is also worth indicating that, Moran's spatial autocorrelation measures the correlation between different variables, but it does not account for the cause of the correlation. Therefore, the spatial factors influencing the correlation, between the mounds, cannot be determined from the statistical analysis. Further detailed analysis is needed to explain this.

6.1.2. Spatial distribution of termite mounds (Density distribution).

The results from the density map of the termite mounds show high to medium density of termite mound distribution in most of the research area. The high density of termite mounds at location (A) Figure 7, suggest that the termites are competing for a particular resource, at that location, as realised in similar studies by (Grohmann et al., 2010; Lee, 1971). This resource could be abundance of moisture in the subsurface or high accumulation of weathered clay products. The high to medium density of the termite mounds also indicates clustering within the distribution of the mounds. The clustering suggests that the distribution of the mounds is not as a result of random chance, as indicated by previous studies (Collins, 1981; Jean-pierre et al., 2015), and also from the spatial distribution of the termite mounds (section 6.1.1). Although the results from previous studies used a method proposed by (Collins, 1981), which took into account one species of the termite. However, the results from this research employed the kernel density distribution from ArcMap 10.5.1, which summed all the mounds of the different species together.

6.1.3. The relationship between the mound directional trends and aeromagnetic data.

From the relationship between the mound directional trend and the aeromagnetic imagery (Figure 11), it is clear the structures suggested by the aeromagnetics have a Hercynian orientation (NE-SW), which is similar to the general trends of the termite mounds (NE-SW). This Hercynian orientation, according to the aeromagnetic image exhibit some very high magnetic anomalies. This also suggests that the mounds are following some high anomalously magnetic defined structures in the research area. These structures could be related to dykes, or some magnetic bodies. The narrow-bounded nature of the magnetic anomalies suggests dyke like intrusions, along this orientation. Further detailed modelling of the binary aeromagnetic data, may be necessary to define the structures that the mounds are following clearly. It is worth noting that, the, binary aeromagnetic data was not available for this research. The lineation and trend (NE-SW) of the aeromagnetic anomalies suggest that structures in the research area are magnetic in nature. This is however not surprising, since according to Leube, et al., (1990), structures within the birimian orogenic terrains are mostly oriented in the Northeast, Southwest (NE-SW) direction. This could, however, mean that the termites are targeting weathered dyke/ intrusive materials and/or moisture, hence the NE-SW alignment with the structural directions within the research area.

6.1.4. The relationship between the mound directional trend and chargeability.

The relationship between the chargeability and the directional trend of the termite mounds Figure 12, shows the orientation of high chargeability areas in the Northeast southwest direction, which the termite mounds seem to follow. This supports the interpretation that the termite mounds distribution is structurally controlled. This is further supported by the highly positive correlation between the mounds and the semi-circular chargeability anomaly in the north of the research area Figure 12. A possible explanation for this behaviour is that the termites are targeting possibly weathered clay, and/or moisture. According to Yatini, Santoso, Læsanpura, & Sulistijo, (2016), the presence of clay and moisture increases chargeability exponentially. The association of the termites with zones of high chargeability could be employed to locate hydrothermal alteration zones, associated with weathered clay, and pyrite within the research area, since sulphides, and clay yield high chargeability within the subsurface (King, 2007; Yatini et al., 2016).

6.1.5. The relationship between the mound directional trend and published major faults.

From the relationship between the published major faults and the directional trends, Figure 13, a north-northeast trend is seen in the south-eastern section of the study area, (A-A). To the east, and the west, a north-northwest, trend (B-B, C-C), and (D-D) respectively Figure 13. The observed trends (B-B, C-C and D-D), is seen to cut across the significant Hercynian fault trends (major faults) Figure 13. Some termite mounds directly correlate with the major faults. The observed trends (B-B, C-C, and D-D) in Figure 13, is seen not to have any correlation with the major faults in the research area. The directional trends (B-B and C-C) is seen to occur around a complex fault system. The orientation of this unusual trend could be related to some fractures or faults, which are not visible from the published major fault, probably due to the resolution of the fault map. The association of the termite mound trends with the major fault and fault trends suggest the termites are targeting structurally controlled resources. These resources could be weathered products such as clay, or moisture, associated with brittle geologic materials within the fault zones: brittle geologic materials are considerably more vulnerable to weathering, in view of their large surface area to volume proportion (Hirth & Hovius, 2005).

6.1.6. The relationship between the mound directional trend and the published geology.

The relationship between the mounds directional trend and the geology was accessed. The result is presented in Figure 27. From the results, it could be seen that most of the mounds are located at or close to the contact between the intrusives and the sediments. The termite mounds could also be seen dominated within the sediments (D). The north-northwest trend of the termite mound in the south-eastern portion of the research area (A), could be seen correlating with the lithological contact between the intrusive and the sediment (E). Also, some of the north-western directional termite mound trends could be seen dominated within the sediments (B), and the intrusive (C). The dominance of the termite mounds within the sediments, and at or close to the contact between the sediments and the intrusive, is not surprising because, at the contact between the intrusive and the sediments, contact metamorphism could make rocks within such zones weathered, and hence weak. Weak here is referred to as "the domain of hard-soil/soft-rocks" (Nickmann, Spaun, & Thuro, 2006). Generally, the association of the termite mounds with the lithological contacts, suggests the termites are targeting weak geological materials, such as weathered clay products. The weathered clay products, seem to be a target for the termites since the termites use these clay products to construct their mounds (Harris, 1956). It has also been noted by Harris, (1956), that some termites also feed on soil nutrients and construct their mound with the by-product. It could also be argued out that, there could be possible shearing at the contacts of the intrusive and the sediments, causing the presence of weak rocks and structures, which the termites are taking advantage of. It is possible the termites are targeting such soft sediments because according to Mège & Rango, (2010), the termite cannot tunnel through competent bedrock, they, consequently, tunnel through weak geological structures.

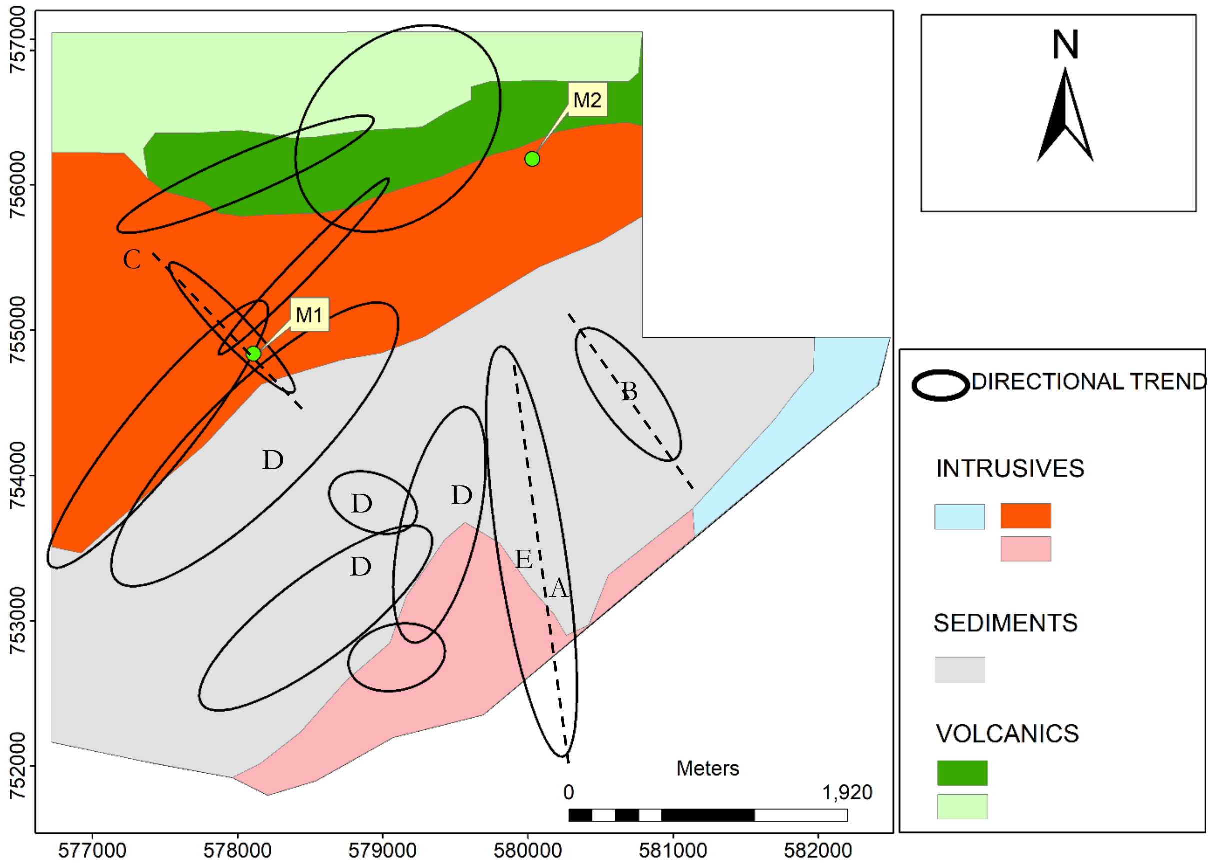

Figure 27. The directional trend of termite mounds and interpreted geology from the regional geologic map of Tepa (Pelangio Resources, 2015). M1 and M2 are mounds studied in detail.

6.1.7. The relationship between density distribution of mounds and published geology.

From the relationship between the published geology and the termite mound density it could be observed that, at the contact between the sediment and the intrusive, there is a high-density of the termite mounds (C) Figure 28. This suggests the termites are competing for a particular resource, which may not be readily available at other parts of the research area since only a medium to low density is observed at those portions (D2, D1, and E) Figure 28. Also, the medium density of the mounds could be observed at or close to the contact between the sediments and the intrusives in the western portion of the research area (D1) and the south-eastern flanks (D2). Generally, most of the termite distribution is seen to be high at or near the contact between the sediments and the intrusive. In the northern section of the research area, a medium density of the mounds could be observed forming a semicircle, close to the contact between different volcanic rocks (E).

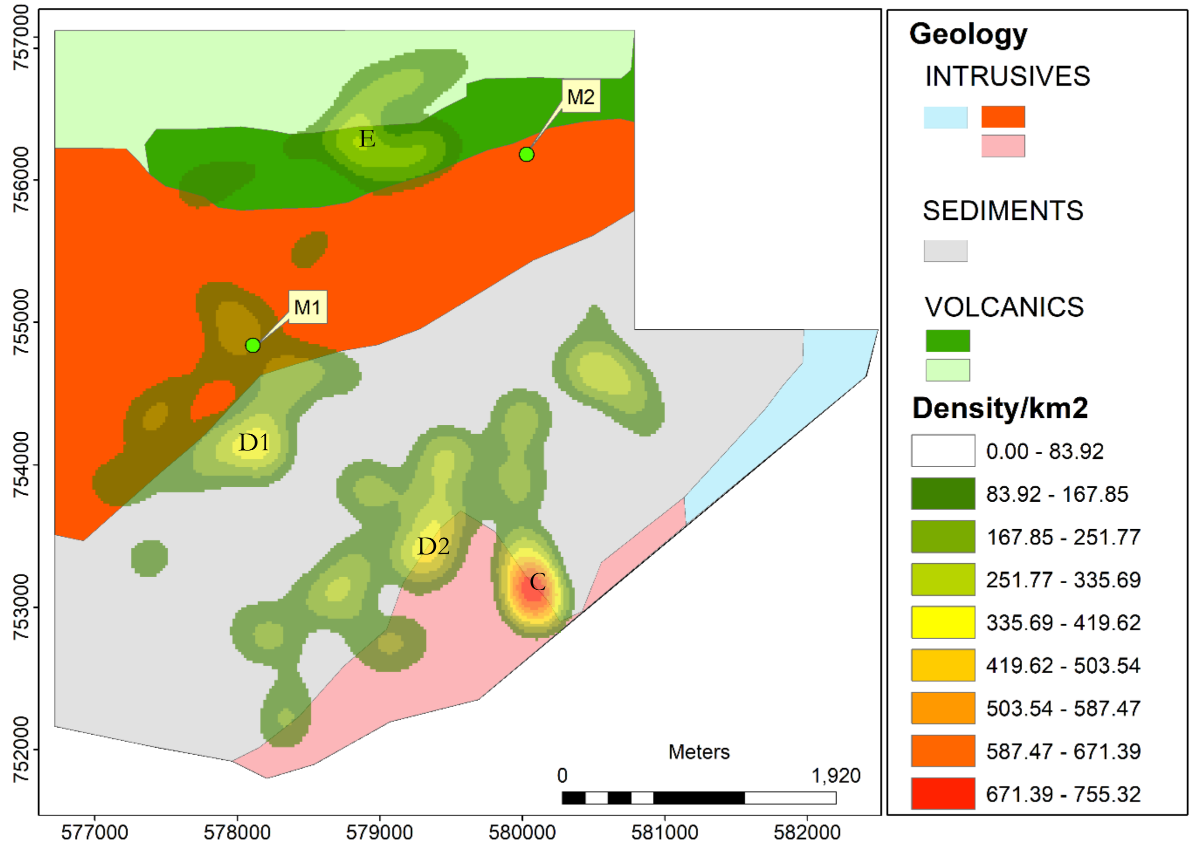

Figure 28. Spatial density of termite mounds superimposed on the regional geology of the research area (Pelangio Resources, 2015) M1 and M2 mounds studied in detail.

6.1.8. The relationship between the directional trend of termite mounds, geology and gold mineralisation.

The directional trend of the termite mounds were superimposed on the geology, and gold (Au) mineralisation both from drill holes and the regolith (Pelangio Resources, 2015). The result is presented in Figure 29. From the results, a very good association between the mound, the sediments, and Au mineralisation both from the regolith and the drill holes could be seen. The north-western termite trend (B, B) is seen to have a positive correlation with the drill hole and the regolith gold (Au) response. Some of the termite mound trends are seen to correlate well with the Au response, especially from the drill holes. The nature of the occurrence of the Au within the research area, suggests a disseminated form of mineralisation, within the structures, although it could not be confirmed from the elemental analysis. The termites seem to be targeting these disseminated deposits probably because of possibly weathered products such as clay as a result of weathering within such deposits. To the west of Figure 29, the termites seem to accumulate within the volcanic and at the contact between the volcanic and the sediments, at a zone that has been targeted by Pelangio Resources for further research due to good response from surface geochemical results. This could suggest the possibility of using the termite mound trend, and density to target zones of plausible mineralisation, during the initial stages of exploration.

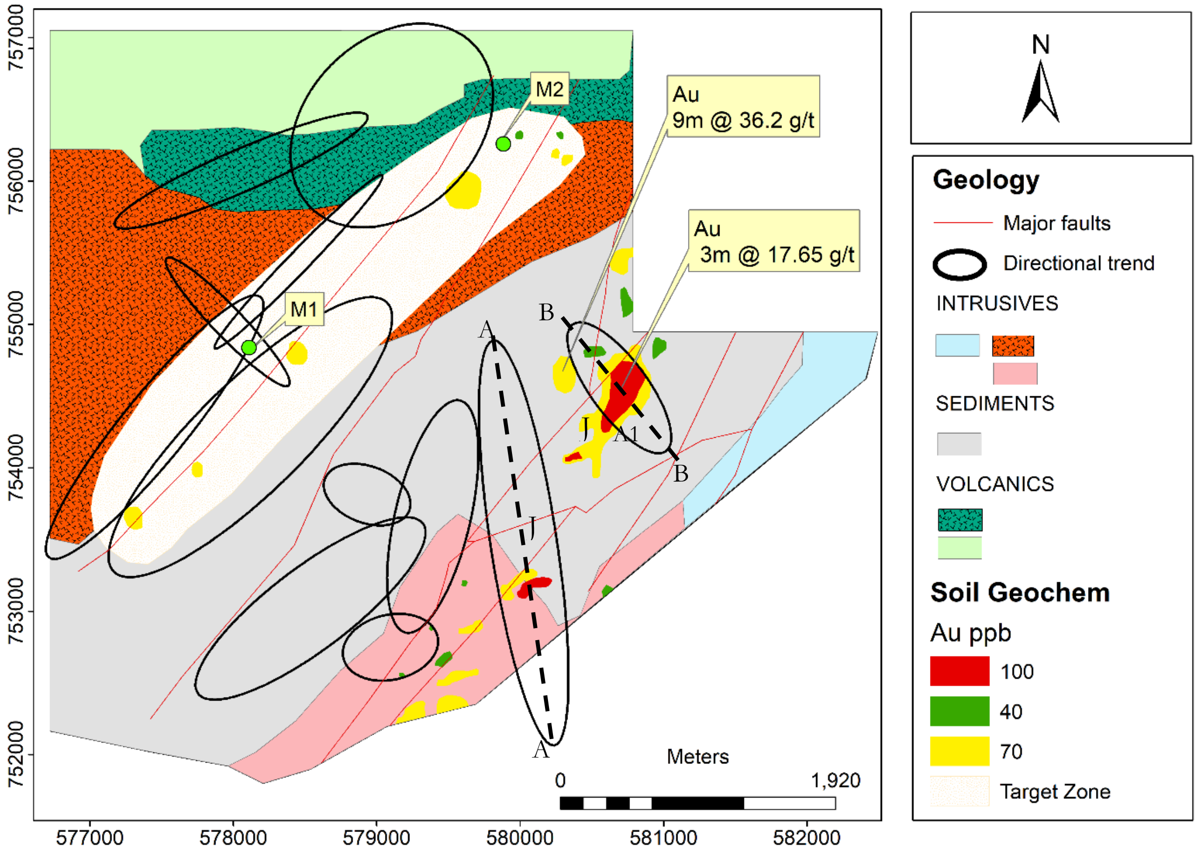

Figure 29. The directional trend of termite mounds superimposed on the geology and Gold (Au) mineralisation, both from the regolith and drill holes. The location of the two termite mounds studied for detailed geochemistry, M1 and M2, are shown.

6.2. Mineralogy and Elemental analysis of the two selected termite mounds.

6.2.1. The crystallinity of kaolinite within the two selected termite mounds.

The diffractograms from the XRD inferred kaolinite, from the two termite mounds, and the immediate subsurface shows similar intensities of the diffractograms, compared to the crystalline reference kaolinite at 2(θ) 20.139° (A), 2(θ) 21.062° (B), and 2(θ) 21.581° (C), see Figure 16, except two missing peaks at 2(θ) 23.197° (E) and 2(θ) 23.774° (F), which represents the amorphous nature of the kaolinite, hence suggesting only partly crystallized/disordered kaolinite (Artioli et al., 1995). The crystallinity index of the two termite mounds (M1 and M2) was additionally estimated to be 75% and 78% respectively. The similarities between the diffractograms of the two termite mounds suggest the termites are sampling similar kaolinite-rich material from the subsurface to build their mounds. The amorphous nature of the kaolinite from the two termite mounds could be attributed to either loss of water from the mineral or the presence of silica or amorphous alumina (Insley & Ewell, 1935). It could also mean that the clay mineral kaolinite might have lost the two peaks (amorphous), due to surface regolith processes, or transportation from the subsurface to the surface. It could also be argued out that the termite's bioturbation activities could have caused the clay to be partly disordered, hence needs further investigation.

The kaolinite from the VNIR-SWIR spectroscopy shows an asymmetric doublet structure in the 2.2 and the 1.4 um region. In particular, a steep minima shoulder at the 2.1650 um doublet structure is observed. The steep minima shoulder and the asymmetric doublet structure indicates decreasing order in the crystal structure of the kaolinite (Spectral international INC, 2018). This finding supports the partly crystallised/disordered kaolinite from the XRD results, which supports the fact that the mineral kaolinite has undergone some surface regolith processes within the transported cover, which has modified the structure of the mineral. From the XRD and the VNIR-SWIR spectroscopy results, it can be concluded that the kaolinite mineral within the two termite mounds is partially crystalised (ordered) but does not include altered kaolinites such as dickite, and nacrite. Hence their provenance can be attributed to semi-residual environment.

6.2.2. Variation of the major elements and gold within the two selected termite mounds and the subsurface.

The results from the ICP-OES elemental analysis indicates that the major elements (Mg, K, Al) within the mounds and the subsurface are below the average crustal concentrations (Barth, 1962). From the ICP-OES elemental results, it could be seen that magnesium (Mg) is very low in concentration both within the two termite's mounds and the subsurface. The low concentration of Mg, suggests that Mg may not be present in high concentration at the location of the two termite mounds. However, comparing the average concentration of Mg in termite mound 1(M1), and termite mound 2 (M2), Figure 19 and Figure 20 respectively, it could be realised that M1 has a relatively high concentration of Mg compared to M2. The difference in the Mg concentration could be related to the different environments which the mounds are located. This, however, needs further investigation. The presence of the element (Mg) in the subsurface is seen to be expressed in M1 and M2, although the concentration of Mg in the subsurface, as stated earlier is below the average crustal concentration. The highest concentration of the element in the two mounds is seen to be expressed at the sides and the apex of the mounds, and less within the Fungus chamber. This indicates that the presence of the elements in the mound is heterogeneous, and therefore, cannot be directly related to the location of the elements in the subsurface. However, the concentration of the Mg at the apex of the mound could be seen partly correlating with the concentration of Mg in the subsurface.

From Figure 21 and Figure 22, representing potassium from termite mounds M1 and M2, it is clear that the high concentration of potassium (K) in the subsurface of M1 is not much expressed within the mound Figure 21. Potassium (K) in M2 is seen almost at zero (0) concentration both within the subsurface and the mound Figure 22. The extreme variation of K observed suggests that the termites may have preference for specific elements, e.g. Aluminium, or particular mineral, that has not much association with potassium. Comparatively, K concentration in M1 is higher than K concentration in M2. From Figure 22, a moderate concentration of K could be seen in the fungus chamber, which is seen to be very low in the immediate subsurface, this indicates that, there is an external source of potassium enrichment, that the termites are sampling from.

From Figure 23 and Figure 24, representing aluminium (Al) within M1 and M2 respectively. Al is expressed in high concentration within the subsurface of M1 and M2, which is relatively expressed in average concentration within termite M1 Figure 23, and less in the fungus chamber. This is however different for M2 Figure 24, where aluminium is found in high concentration within the subsurface but expressed in a very low concentration within the mound. The source of the high concentration of Al within the subsurface can be attributed to the mineral kaolinite. This is because Al forms an integral component of kaolinite and the mineral (kaolinite) has been found in high abundance both within the subsurface and the two termite mounds (see Appendix 1, to 1.5). Also, from Figure 27, the two termite mounds can be located within the granitic intrusive. According to the published regional geology (Pelangio Resources, 2015), a common weathered product from feldspar bearing granite is kaolinite. There is the possibility that the granite maybe weathered, hence the termites sampling from the weathered granite, since the weathering of granite can result in the mineral kaolinite (Grant, 1962).

From Figure 25 and Figure 26, representing the concentration of gold (Au) within M1 and M2. It could be realised that the concentration of Au within the subsurface of both mounds seems to be fairly high but differently expressed within the mounds. This indicates upward migration of the elements into the surficial environment. From Figure 25, M1 shows a high concentration of the Au at the side and apex of the mound, excluding the fungus chamber. This is however different for termite M2, where the high concentration of the Au within the subsurface is sparingly expressed only at the sides of the mound. Generally, termite M1 seem to have high concentration of Au than M2, although comparatively, the subsurface of M2 seems to have high concentration of Au, than M1. This could be related to the different environments of the two mounds, a possible explanation is that, from Figure 28, M1 is located within an area where there is an average density of 460 mounds per square kilometre, indicating semi clustering whilst M2 is seen to be isolated, with no mound clustering. The clustering of the mounds suggests the termites are competing for resources (weathered clay and or moisture), and according to Mege, (2010), the termites build tunnels in geological structures, because they cannot burrow through hard rocks. This suggests the termites are sampling weathered clay products from either a fault zone or a dyke, and that there is the possibility of concentration of Au within such environment, hence the high concentration within M1. The concentration of Au within the two termite mounds is consistent with research conducted by Stewart et al., (2012), in Western Australia, where high concentration of Au was found in termite mounds. The concentration of Au within the two termite mounds, however, does not mean the termites necessarily transport Au to the surface. They rather transport clay materials, lithic rock fragments and water for their mound construction, and if these elements happen to be within the trajectory of the termites, they may, however, be carried along to the surface for the construction of the mound. The presence of the Au and the partially disordered kaolinite from both termite mounds and their immediate subsurface (section 6.2.1) possibly suggest a supergene enrichment, within the residual regolith environment.

The average concentration of the elements within the mounds and the subsurface were found to vary between 0.01 and 2068 mg/kg for potassium, 349 and 1016 mg/kg for magnesium, 36306 and 116260 mg/kg for aluminium, and 0.01 and 156 mg/kg for gold. The highest concentration was found within the subsurface, with average concentration within the mounds. Although the concentrations of the major element in the mounds, and the subsurface, except gold is below the average crustal abundance of the elements (Barth, 1962), they are found expressed in the mounds in average to medium concentrations.

6.2.3. Correlation between gold (Au), major and trace elements in termite mound 1 and 2 and their immediate subsurface.

The relationship between gold, major and trace elements within termite mounds 1 and 2 and the subsurface was determined using principal component analysis (correlation matrix). The result is presented in Table 5. The result shows two (2) components extracted from the dataset, based on their factor loadings. The factor loadings of the elements in both components have been analysed. The element with the higher factor loading in a particular component has been highlighted in red. From the results, the elements potassium (K), Zinc (Zn), Indium (In), Iron (Fe), and Aluminium (Al) is seen to have high factor loadings with gold (Au), in component 1. The elements Magnesium (Mg) and Calcium is seen to have high factor loadings in component 2. The association of gold with the elements in component one suggests that gold could be associated more with Zn, In, Fe, and Al, and less with Mg and Ca, within the research area, the elements (K, Zn, In), could serve as pathfinder to gold. This result is in line with research conducted by Arhin et al., (2015), where Zn was identified as pathfinder element for Au within termite mounds. The type of deposit within the research area, from the regional geology map, reveals an orogenic structurally controlled Au deposit. However, this could not be determined, because there are not enough elements, and detailed alteration, mineral/zonation information supplied to properly classify the deposit. However, the two components extracted from the factor analysis could suggest the variations in the lithology of the research area, based on the elemental association.

Table 5. Correlation matrix of gold, major and trace elements.

Component Matrix[a]		
	Component	
	1	2
Mg	0.590	0.600
K	0.019	-0.868
Zn	0.840	-0.137
In	0.954	0.129
Ca	-0.510	0.513
Fe	0.928	-0.109
Al	0.976	-0.040
Au	0.464	0.122

6.2.4. Characterising the subsurface with Geochemistry.

The subsurface regolith was classified, using the ratio of the relatively mobile element Al, to the relatively immobile elements Mg and K. This is plotted in a model proposed by McQueen, (2006). The model plots the ratio of the elements (Mg/Al) on the Y-axis and (K/Al) on the X-axis. This helps to classify the sources of geological regolith materials into saprolite, relict, ferruginous, or transported clay sediments and further classifies the materials into the major mineralogical components, based on the quadrants which they plot in. The result is presented in Figure 30 and further zoomed in Figure 31. Figure 30, shows that, samples from the two termite mounds and their subsurface plot in the transported clay sediments quadrant. This indicates, there is no major difference between the two mounds and the subsurface in terms of the regolith. This suggests the possibility of using the termite mounds to characterise their immediate subsurface.

According to Nude & Arhin, (2009), the soil geochemical sample should reflect the underlying geology if in-situ, therefore if the termites are sampling from an in-situ substrate, the mound sample should not be different from the subsurface substrate. It can also be seen that the termite mounds and the subsurface materials within the transported clay sediments quadrant correlates well with the clay mineral kaolinite, as can be seen in Figure 30, which is confirmed from the XRD analysis, and the VNIR-SWIR spectroscopy Figure 16 and Figure 18. This could indicate that the termites are sampling from the transported weathered environment. From Figure 31, variation within the sediments in the transported clay sediment quadrant could be observed; this is however, beyond the scope of this research. The presence and association of Au with the partially crystalline kaolinite suggest there is possible supergene enrichment. It is worth noting that, from literature, the termites are supposed to sample the geology in a way, but the characterisation of the subsurface using the mounds suggests the termite are sampling from the regolith environment. The possible explanation is that lateritic caps beneath the regolith, could serve as false bed rock and can hence restrict the burrowing activities of the termite within the regolith.

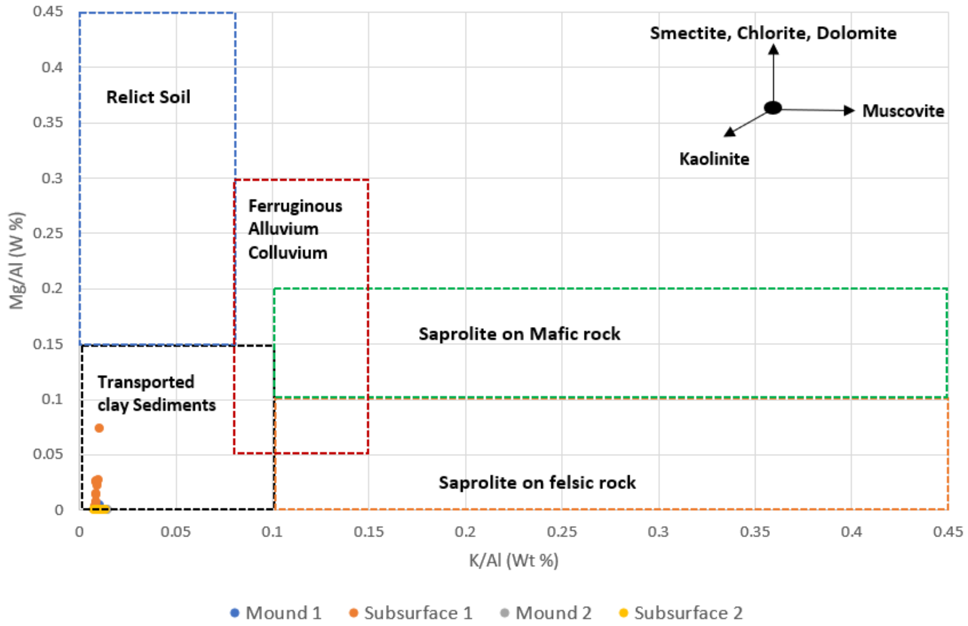

Figure 30. K/Al vs Mg/Al ratio plot percent weight for subsurface of termite mound 2.

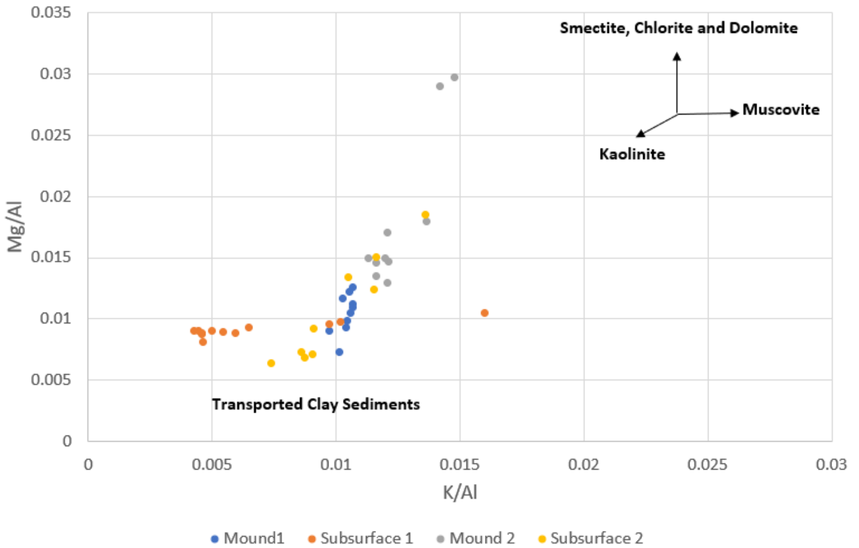

Figure 31. The zoomed plot of the transported clay sediment quadrant, showing variations within the transported sediments.

7. CONCLUSION.

7.1. Spatial distribution of termite mounds.

Geophysical investigation as stated earlier provides an excellent means of seeing below the transported cover. However, the cost of investigation and in particular mobilisation makes it difficult for upcoming mining companies to use this method. This study suggests an alternate means of characterising the subsurface, using the spatial distribution, supported by the geochemistry of termite mounds. This study confirms that termite mounds are not randomly distributed within the research area, and that, there is a spatial factor influencing the distribution of the mounds. It further suggests that termites source for weathered clay products, and moisture from geologically weak zones, especially from fault zones and dykes, thereby orienting their mounds either on or close to such zones, beyond the transported cover. The spatial distribution of termite mounds can, therefore, be used to infer the presence of near-surface structures such as faults, lithologic contacts, and structurally controlled chargeability zones. However, the distinction between these structures and lithological contacts will be difficult to tell, with this type of method. This is because the termites, cannot distinguish between different geologic zones. In other words, the termite mound characterisation of the subsurface gives a bulk characterisation, with preference for clay-bearing most weak subsurface zones.

7.2. Geochemistry of termite mounds.

This study has also demonstrated that the mineralogy as determined by the XRD and ASD-SWIR spectroscopy of termite mounds is not different from the mineralogy of the immediate subsurface of the mounds. Hence the study shows the possibility to characterise the major subsurface minerals and regolith materials in the immediate environment of termite mounds using the geochemistry of the mounds. The average concentration of the elements within the subsurface was found to be expressed heterogeneously within the mounds. This study has proven the possibility of using the termite mound geochemistry to characterise the immediate subsurface regolith. The partial crystallinity of the kaolinite from the two termite mounds suggested that its source can be related to a semi residual environment, within the research area. Also, the anomalous concentration of gold within the immediate environment of the mound was expressed in the mound, in average to medium concentration. This indicates the capability to use these mounds as a proxy for mineral exploration.

7.3. Recommendation.

During the course of this research, it was realised that, there has not been much research into using the spatial distribution of the termite mounds and their geochemistry to image the subsurface, therefore, further fieldwork from different environments is recommended to help establish the efficacy of this method.

One significant issue realized was that, from literature, the termites must sense the geology undercover somehow, but the characterisation of the subsurface using the mound sample reveals only sediments and minerals in the subsurface of the regolith. This however needs further investigation.

Additionally, the possible effect of termite bioturbation on the crystallinity of kaolinite needs to be further investigated.

The use of satellite imagery with a high spatial resolution such as Digital globe or Quick bird is recommended to map the spatial distribution of the mound, if similar research is repeated in an arid environment.

8. REFERENCES.

Affam, M. and Arhin, E. (2005). Termite Mound-A Supplementary Geochemical Gold Sampling Medium in Complex Regolith Terrain. *Ghana Mining Journal*, (8), 10–15.

Ali, I. G., Ahmed, B. M. S., Sheridan, G., & French, J. R. J. (2016). The Effect of Termite Activity on Soil Profile in a Laboratory Test Tank, *9*(12), 97–108. https://doi.org/10.9790/2380-09120297108.

Allibone, A., Hayden, P., Cameron, G., & Duku, F. (2004). Paleoproterozoic Gold Deposits Hosted by Albite- and Carbonate-Altered Tonalite in the Chirano District, Ghana, West Africa. *Economic Geology*, *99*(3), 479–497. https://doi.org/10.2113/gsecongeo.99.3.479.

Anand, r.R., Smith, R.E., Phang, C., Wildman, J.E., Robertson. I.D.M and Munday, T. J. (1993). *Geochemical exploration in complex lateritic environments of the Yilgarn Craton, Western Australia. Report 442R, CSIRO Division of Exploration and Mining, Perth,.*

Anand, R. R., Aspandiar, M. F., & Noble, R. R. P. (2016). A review of metal transfer mechanisms through transported cover with emphasis on the vadose zone within the Australian regolith. *Ore Geology Reviews*, *73*, 394–416. https://doi.org/10.1016/j.oregeorev.2015.06.018.

Arhin, E., Boadi, S., & Esoah, M. C. (2015). Identifying pathfinder elements from termite mound samples for gold exploration in regolith complex terrain of the Lawra belt, NW Ghana. *Journal of African Earth Sciences*, *109*, 143–153. https://doi.org/10.1016/j.jafrearsci.2015.05.022.

Arhin, E., & Nude, P. M. (2010). Use of termitaria in surficial geochemical surveys: evidence for >125- m size fractions as the appropriate media for gold exploration in northern Ghana. *Geochemistry: Exploration, Environment, Analysis*, *10*(4), 401–406. https://doi.org/10.1144/1467-7873/09-004.

Arhin E., and N. P. M. (2009). Significance of regolith mapping and its implication for gold exploration in northern Ghana: a case study at Tinga and Kunche. *Geochemistry: Exploration, Environment, Analysis*, *9*, 63–69.

Artioli, G., Bellotto, M., Gualtieri, A., & Pavese, A. (1995). Nature of structural disorder in natural kaolinites: A new model based on computer simulation of powder diffraction data and electrostatic energy calculation. *Clays and Clay Minerals*, *43*(4), 438–445. https://doi.org/10.1346/CCMN.1995.0430407.

Babiker, M., & Gudmundsson, A. (2004). The effects of dykes and faults on groundwater flow in an arid land: the Red Sea Hills, Sudan. *Journal of Hydrology*, *297*(1–4), 256–273. https://doi.org/10.1016/j.jhydrol.2004.04.018.

Barth. (1962). *Theoretical Petrology* (2nd ed.). New York: John Wiley and Sons, Inc.

Bhunia, G. S., Kesari, S., Chatterjee, N., Kumar, V., & Das, P. (2013). Spatial and temporal variation and hotspot detection of kala-azar disease in Vaishali district (Bihar), India. *BMC Infectious Diseases*, *13*(1), 64. https://doi.org/10.1186/1471-2334-13-64.

Bland, J. M., & Altman, D. G. (1996). Statistics notes: Measurement error. *BMJ*, *312*(7047), 1654–1654. https://doi.org/10.1136/bmj.312.7047.1654.

Butt, C.R.M., Gray, D.J., Robertson, I.D.M Lintern, M.J., Anand, R.R., Britt, A., Bristow, A.P.J., Munday, T.J., Phang, C., Smith, R.E., Wildman, J.E, . 1997. (1997). AMIRA P409-Yildan Transported Overburden Final Report. *CSIRO Division of Exploration and Mining Restricted Report 333R,* 164.

Butt, C. R. M., Lintern, M. J., & Anand, R. R. (2000). Evolution of regoliths and landscapes in deeply weathered terrain — implications for geochemical exploration.

Chakravarthy, A. K., & Sridhara, S. (2016). *Economic and ecological significance of arthropods in diversified ecosystems: Sustaining regulatory mechanisms*. *Economic and Ecological Significance of Arthropods in Diversified Ecosystems: Sustaining Regulatory Mechanisms*. https://doi.org/10.1007/978-981-10-1524-3.

Clark, R. N. (1999). Spectroscopy of rocks andminerals, and principles of spectrocopy. *Remote Sensing for the Earth Sciences: Manual of Remote Sensing*, *1*, 3–58.

Collins, N. M. (1981). Populations, Age Structure and Survivorship of Colonies of Macrotermes bellicosus (Isoptera: Macrotermitinae). *The Journal of Animal Ecology*, *50*(1), 293. https://doi.org/10.2307/4046.

Consulting, S. (2013). *Mineral Resource Evaluation Technical Report , Manfo Gold Project , Manfo Gold Project ,.* Canada.

Cosarinsky, M. I. (2011). The Nest Growth of the Neotropical Mound-Building Termite, Cornitermes cumulans : A Micromorphological Analysis. *Journal of Insect Science*, *11*(122), 1–14. https://doi.org/10.1673/031.011.12201.

Coventry, R.J., Holt, J.A. and Sinclair, D. F. (1988). Nutrient cycling by mound-building termites in low-fertility soils of semi-arid tropical Australia. *Australian Journal of Soil Research*, *26*, 375–390.

Croghan, C. A. P. P. E. (2003). Methods of Dealing with Values Below the Limit of Detection using SAS. In *EPA Science Inventory* (p. 5). St. Petersburg, FL: Southeastern SAS User Group.

Cudahy, T. (1997). *PIMA-II spectral characteristics of natural kaolins*. *Amira Project*. North Ryde, Australia.

Eggleton, P. (2000). Global patterns of termite diversity. In M. H. Abe, D.E. Bignell (Ed.), *Termites: evolution, sociality, symbioses, ecology* (pp. 25–51). Dordrecht: Kluwer Academic Publishers.

Eggleton, P. (2010). An introduction to Termites: Biology, Taxonomy and functional Morphology. *Springer, Dordrecht.*

Erdemoğlu, M., & Baláž, P. (2012). An Overview of Surface Analysis Techniques for Characterization of Mechanically Activated Minerals. *Mineral Processing and Extractive Metallurgy Review*, *33*(1), 65–88. https://doi.org/10.1080/08827508.2010.542582.

Forsyth, j. (1966). Agricultural insects of Ghana. In *Agricultural insects of Ghana* (pp. 76–78). Accra: Accra: Ghana University press.

Gandhi, S. M., & Sarkar, B. C. (2016). *Essentials of mineral exploration and evaluation*. Saint Louis: Elsevier Science.

Getis, A., & Ord, J. K. (1992). The Analysis of Spatial Association by Use of Distance Statistics. *Geographical Analysis*, *24*(3), 189–206. https://doi.org/10.1111/j.1538-4632.1992.tb00261.x

Gleeson, C.F. & Poulin, R. (1989). Gold exploration iin niger using soils and termitaria. *Journal of Geochemical Exploration*, *31*, 253–283.

Grant, W. H. (1962). Weathering of Stone Mountain Granite. *Clays and Clay Minerals*, *11*(1), 65–73. https://doi.org/10.1346/CCMN.1962.0110106.

Grigg, G. C., & Underwood, A. J. (1977). An analysis of the orientation of "Magnetic" termite mounds. *Australian Journal of Zoology*, *25*(1), 1–7. https://doi.org/10.1071/ZO9770087.

Grohmann, C., Oldeland, J., Stoyan, D., & Linsenmair, K. E. (2010). Multi-scale pattern analysis of a mound-building termite species. *Insectes Sociaux*, *57*(4), 477–486. https://doi.org/10.1007/s00040-010-0107-0.

Harris, W. V. (1956). Termite mound building. *Insectes Sociaux*, *3*(2), 261–268. https://doi.org/10.1007/BF02224306.

Henckens, M. L. C. M., van Ierland, E. C., Driessen, P. P. J., & Worrell, E. (2016). Mineral resources: Geological scarcity, market price trends, and future generations. *Resources Policy*, *49*, 102–111. https://doi.org/10.1016/j.resourpol.2016.04.012.

Hesse, P. R. (1955). A Chemical and Physical Study of the Soils of Termite Mounds in East Africa. *The Journal of Ecology*, *43*(2), 449. https://doi.org/10.2307/2257006.

Hinze, W. J., Frese, R. R. B. von, Frese, R. Von, & Saad, A. H. (2013). *Gravity and Magnetic Exploration: Principles, Practices, and Applications*. https://doi.org/10.1017/CBO9780511843129.

Hirth, G., & Hovius, N. (2005). *Tectonic Faults Agents of Change on a Dynamic Earth*. (M. R. HANDY & A. N. H. GREG HIRTH, Eds.). Berlin: Library of Congress Cataloging.

Insley, H., & Ewell, R. H. (1935). Thermal behavior of the kaolin minerals. *Journal of Research of the National Bureau of Standards*, *14*(5), 615. https://doi.org/10.6028/jres.014.037.

J.C. Gower. (1985). Properties of Euclidean and Non-Eucllidean Distance Matrices. *Elsevier Science*, 81–97.

Jackson, P. D. (1975). An electrical resistivity method for evaluating the in‐ situ porosity of clean marine sands. *Marine Geotechnology*, *1*(2), 91–115. https://doi.org/10.1080/10641197509388156.

Jackson M. I. (1956). *Soil Chemical Analysis-Advanced course* (2nd ed.). Wisconsin: Professor Jackson Madison.

Jayawickreme, D. H., Jobbágy, E. G., & Jackson, R. B. (2014). Geophysical subsurface imaging for ecological applications. *New Phytologist*, *201*(4), 1170–1175. https://doi.org/10.1111/nph.12619.

Jean-pierre, B., Moise, A. A. A., Mauricette, O. S., Philippe, K. K., & Ahoua, Y. (2015). Spatial distribution and density of termite mounds in a protected habitat in the south of Cote D'Ivoire: case of national floristic center (CNF) of UFHB of Abidjan. *European Scientific Journal*, *11*(3), 241–259.

Kebede, F. (2004). Use of termite mounds in geochemical exploration in North Ethiopia. *Journal of African Earth Sciences*, *40*(1–2), 101–103. https://doi.org/10.1016/j.jafrearsci.2004.06.002.

Kennedy, M. (2013). *Introducing geographic information systems with ArcGIS : a workbook approach to learning GIS*

(3rd ed.). John Wiley & Sons, Inc., Hoboken, New Jersey. https://doi.org/10.1017/CBO9781107415324.004

King, A. (2007). Review of Geophysical Technology for Ni-Cu-PGE deposits. *Ore Deposits and Exploration Technology*, *1*, 647–665.

Lee KE, W. T. (1971). Termites and Soils. In *Academic Press,* (p. 251). London and New York.

Leube, A., Hirdes, W., Mauer, R., & Kesse, G. O. (1990). The early Proterozoic Birrimian Supergroup of Ghana and some aspects of its. *Precambrian Ore Deposits Related to Tectonics.*, *46*(1–2), 139–165.

Liu, X., Monger, H. C., & Whitford, W. G. (2007). Calcium carbonate in termite galleries - Biomineralization or upward transport? *Biogeochemistry*, *82*(3), 241–250. https://doi.org/10.1007/s10533-006-9067-x.

Lobry De Bruyn, Lisa A, C. (1995). Soil modification by termites in the central wheatbelt of Western Australia. *Australian Journal of Soil Research ·*, *33*(1), 179–193.

Mariita, N. O. (2010). Application of geophysical methods to geothermal energy exploration in Kenya. *Short Course V on Exploration for Geothermal Resources, Organized by UNU-GTP, GDC and KenGen, at Lake Bogoria and Lake Naivasha, Kenya, Oct*, 1–8.

McQueen, K. G. (2006). Unravelling the regolith with geochemistry. *Regolith 2006 - Consolidation and Dispersion of Ideas*, 230–235.

Mege, D. (2010). Survival strategy of Macrotermes subhyalinus on hard rock and fracture porosity aquifers, (January 2008), 1–3.

Mège, D., & Rango, T. (2010). Permanent groundwater storage in basaltic dyke fractures and termite mound viability. *Journal of African Earth Sciences*, *57*(1–2), 127–142. https://doi.org/10.1016/j.jafrearsci.2009.07.014.

Moran, P. A. P. (1950). Notes on Continuous Stochastic Phenomena. *Biometrika*, *37*(1/2), 17. https://doi.org/10.2307/2332142.

Nickmann, M., Spaun, G., & Thuro, K. (2006). Engineering geological classification of weak rocks. *International Association for Engineering Geology and the Environment*, *492*(492), 9.

Norgrove, L., & Hauser, S. (2015). Estimating the Consequences of Fire Exclusion for Food Crop Production, Soil Fertility, and Fallow Recovery in Shifting Cultivation Landscapes in the Humid Tropics. *Environmental Management*, *55*(3), 536–549. https://doi.org/10.1007/s00267-014-0431-7.

Nude, P. M., & Arhin, E. (2009). Overbank sediments as appropriate geochemical sample media in regional stream sediment surveys for gold exploration in the savannah regions of northern Ghana. *Journal of Geochemical Exploration*, *103*(1), 50–56. https://doi.org/10.1016/j.gexplo.2009.06.005.

Nude, P. M., Arhin, E., Yidana, S. M., Foli, G., & Dowuona, G. N. N. (2014). Geochemical Dispersion of Elements and Their Correlation with Gold in the Regolith at the Tetteh Prospect of the Chirano Gold Mines in the Sefwi Belt of the Birimian , Southwestern Ghana. *Journal of Environment and Earth Science*, *4*(9), 1–18.

Obi, J. C., Ogunkunle, a O., & Meludu, N. T. (2008). Effect of termite infestation on the farming system characteristics of an endemic area in the Guinea savanna region of Nigeria. *American-Eurasian Journal of Scientific Research*, *3*(1), 1–6.

Oha, I. A., Onuoha, K. M., Nwegbu, A. N., & Abba, A. U. (2016). Interpretation of high resolution aeromagnetic data over southern benue trough, Southeastern Nigeria. *Journal of Earth System Science*, *125*(2), 369–385.

Park, J., Lee, K. H., Seo, H., Ryu, J., & Lee, I. M. (2017). Role of induced electrical polarization to identify soft ground/fractured rock conditions. *Journal of Applied Geophysics*, *137*, 63–72. https://doi.org/10.1016/j.jappgeo.2016.12.017.

Pelangio Resources. (2015). Outlook for the Manfo Property. Retrieved November 17, 2017, from http://www.pelangio.com/s/manfo.asp.

Prasad, E.A.V. and Vijayasaradhi, D. (1984). Termite mound in geochemical prospecting. *Curr. Sci*, *53*, 649–651.

Sako, A.; Mills, A. J. & Roychoudhury, A. N. (2009). Rare earth and trace element geochemistry of termite mounds in central and northeastern Namibia: Mechanisms for micro-nutrient accumulation. *Geoderma*, *153*(1–2), 217–250.

Sako, A., Mills, A. J., & Roychoudhury, A. N. (2009). Rare earth and trace element geochemistry of termite mounds in central and northeastern Namibia: Mechanisms for micro-nutrient accumulation. *Geoderma*, *153*(1–2), 217–230. https://doi.org/10.1016/j.geoderma.2009.08.011.

Samadder, R. K., Kumar, S., & Gupta, R. P. (2011). Paleochannels and their potential for artificial groundwater recharge in the western Ganga plains. *Journal of Hydrology*, *400*(1–2), 154–164. https://doi.org/10.1016/j.jhydrol.2011.01.039.

Sandström, H., Reeder, S., & Bartha, A. (1998). Sample preparation and analysis. *Geochemical Atlas of* …, 1–14.

Schlüter, T. (2006). *Geological Atlas of Africa: with Notes on Stratigraphy, Tectonics, Economic Geology, Geohazard and Geosites of Each Country*. *Geological Atlas of Africa*. https://doi.org/10.2113/gsecongeo.103.6.1379.

Silverman, B. (1986). Density estimation for statistics and data analysis. *Chapman and Hall*, *37*(1), 1–22. https://doi.org/10.2307/2347507.

Singh, V. P., Singh, P., & Haritashya, U. K. (Eds.). (2011). *Encyclopedia of Snow, Ice and Glaciers*. *Springer* (Vol. 44). Dordrecht: Springer Netherlands. https://doi.org/10.1007/978-90-481-2642-2.

Spectral international INC. (2018, October 6). Clay minerals. Retrieved January 9, 2018, from http://www.spectral-international.com/clay_min.html.

Stewart, A. D., Anand, R. R., & Balkau, J. (2012). Source of anomalous gold concentrations in termite nests, Moolart Well, Western Australia: implications for exploration. *Geochemistry: Exploration, Environment, Analysis*, *12*(4), 327–337. https://doi.org/10.1144/geochem2012-126.

Telford, W., & Sheriff, R. (1990). *Applied Geophysics* (2nd ed.). New York: Cambridge University Press.

Tobler, W. R. (1970). A Computer Movie Simulating Urban Growth in the Detroit Region. *Economic Geography*, *46*, 234. https://doi.org/10.2307/143141.

Turner, J. S. (2000). Architecture and morphogenesis in the mound of Macrotermes michaelseni (Sjostedt) (Isoptera: Termitidae, Macrotermitinae) in northern Namibia. *Cimbebasi*, *16*, 143–175.

Van Reeuwijk, L. P. (2002). *Procedures for Soil Analysis* (6th ed). Wageningen, The Netherlands.: International Soil Reference and Information Centre (ISRIC).

W.V. Harris. (1956). Termite mound building. *Insectes Soc.*, *3*, 261–268.

Warren C. Day, Jane M. Hammarstrom, Michael L. Zientek, and T. P. F. (2016). Overview with Methods and Procedures of the U.S. Geological Survey Mineral-Resource Assessment of the Sagebrush Focal Areas of Idaho, Montana, Nevada, Oregon, Utah, and Wyoming. In and M. L. Z. Warren C. Day, Thomas P. Frost , Jane M. Hammarstrom (Ed.), *Mineral Resources of the Sagebrush Focal Areas of Idaho, Montana, Nevada, Oregon, Utah, and Wyoming* (2nd ed., pp. 2–211). Virginia: U.S. Geological Survey.

Watson, J. A.L., G. (1970). The role of grass-eating termites in the degradation of a mulga ecosystem. *Search*, *1*(1), 43.

Yatini, Santoso, D., Læsanpura, A., & Sulistijo, B. (2016). Influence of physical parameters to time domain induced polarization (TDIP) response. *AIP Conference Proceedings*, *1719*(2016). https://doi.org/10.1063/1.4943705.

Zhou, X., & Lin, H. (2008). Moran's I. In S. Shekhar & H. Xiong (Eds.), *Encyclopedia of GIS* (p. 725). Boston, MA: Springer US. https://doi.org/10.1007/978-0-387-35973-1_817.

9. APPENDIX

9.1. Appendix 1

XRD results of the termite mound samples from mound 1.

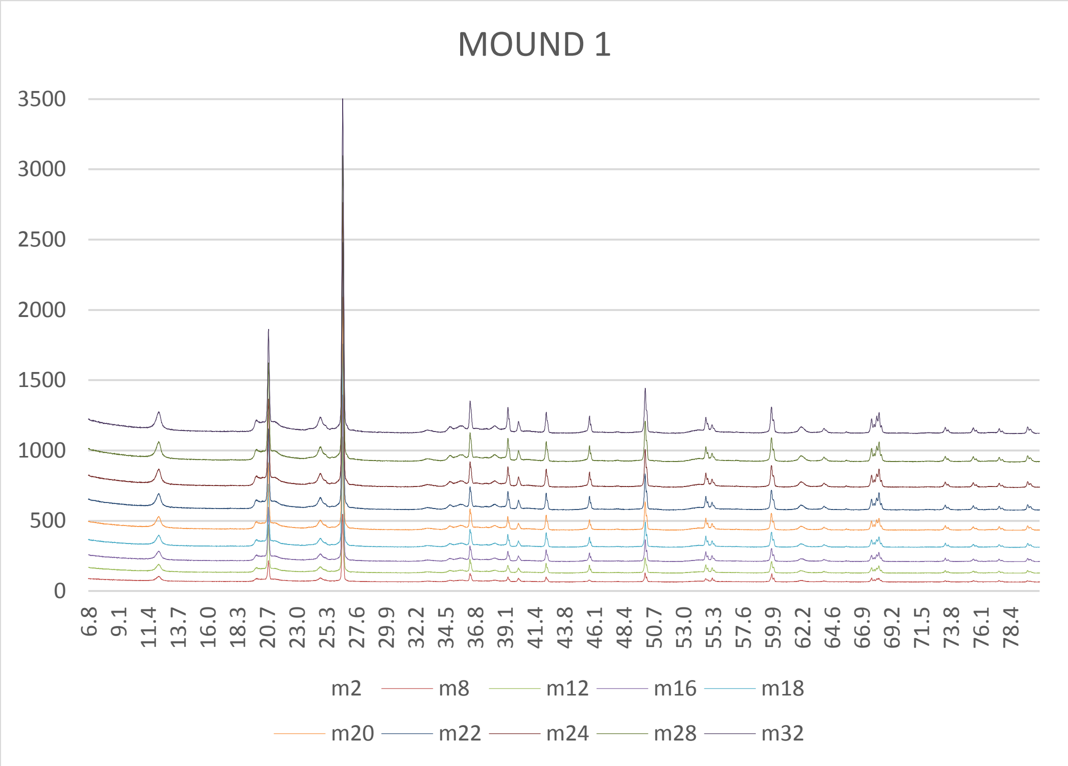

9.2. Appendix 1.1

XRD results from the immediate subsurface of mound 1.

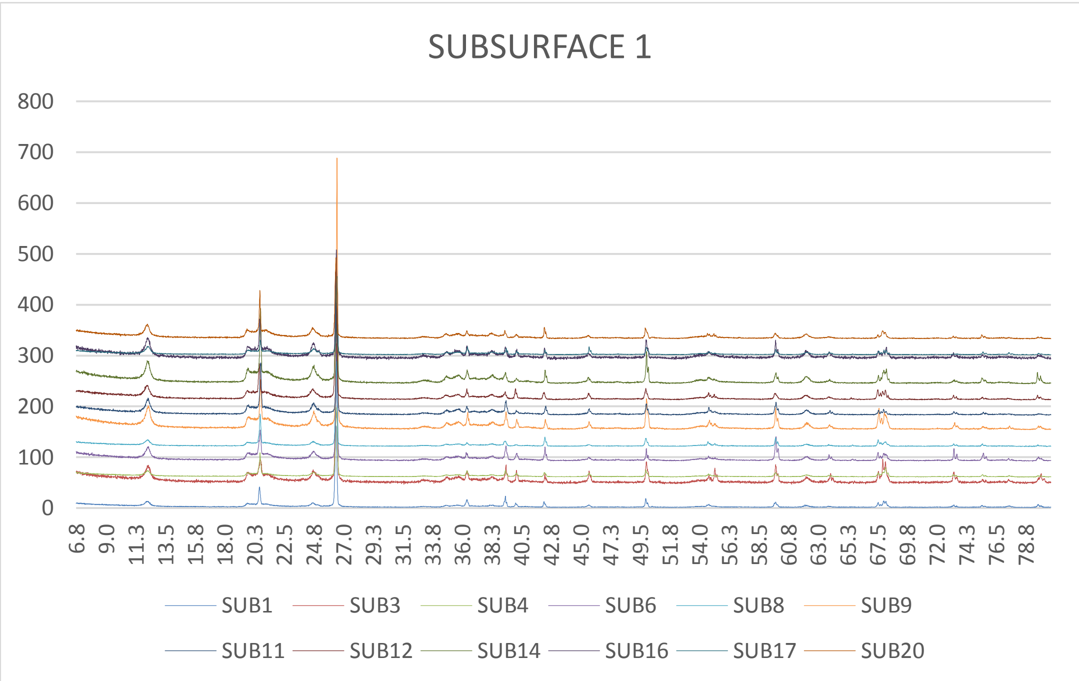

9.3. Appendix 1.2

XRD results of the termite mound samples from mound 2.

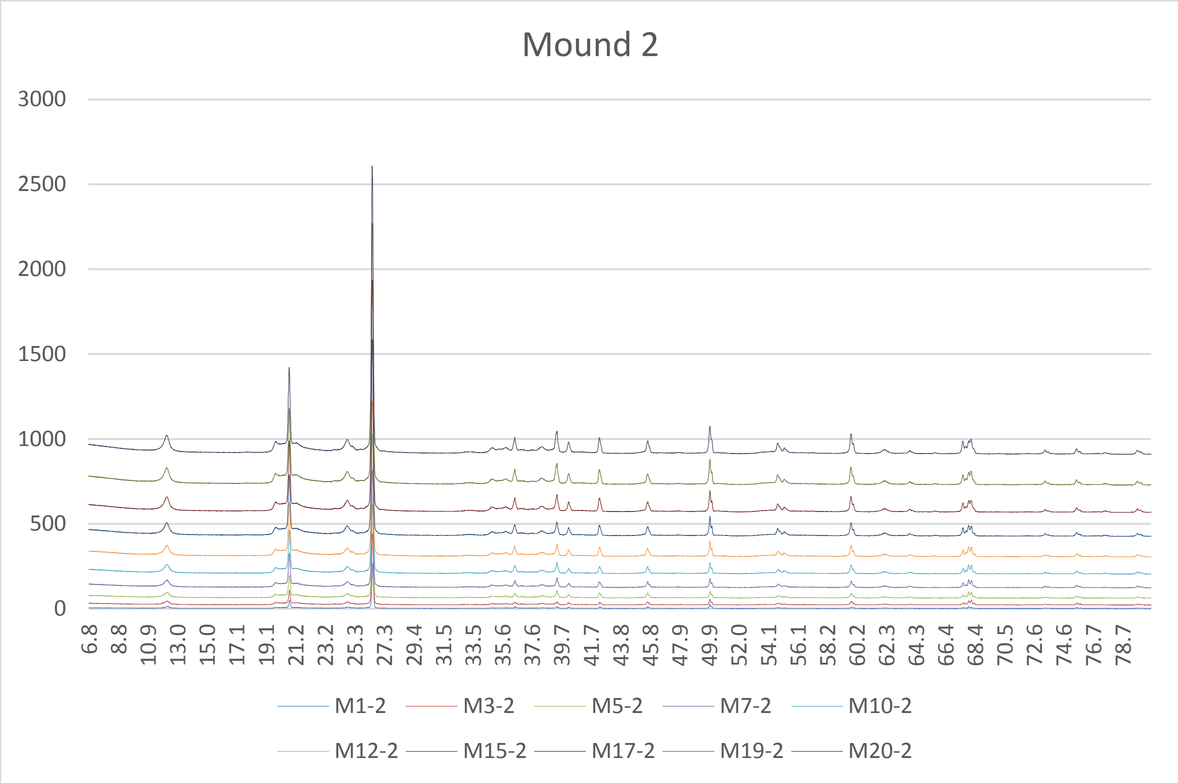

9.4. Appendix 1.3

XRD results from the immediate subsurface of mound 1.

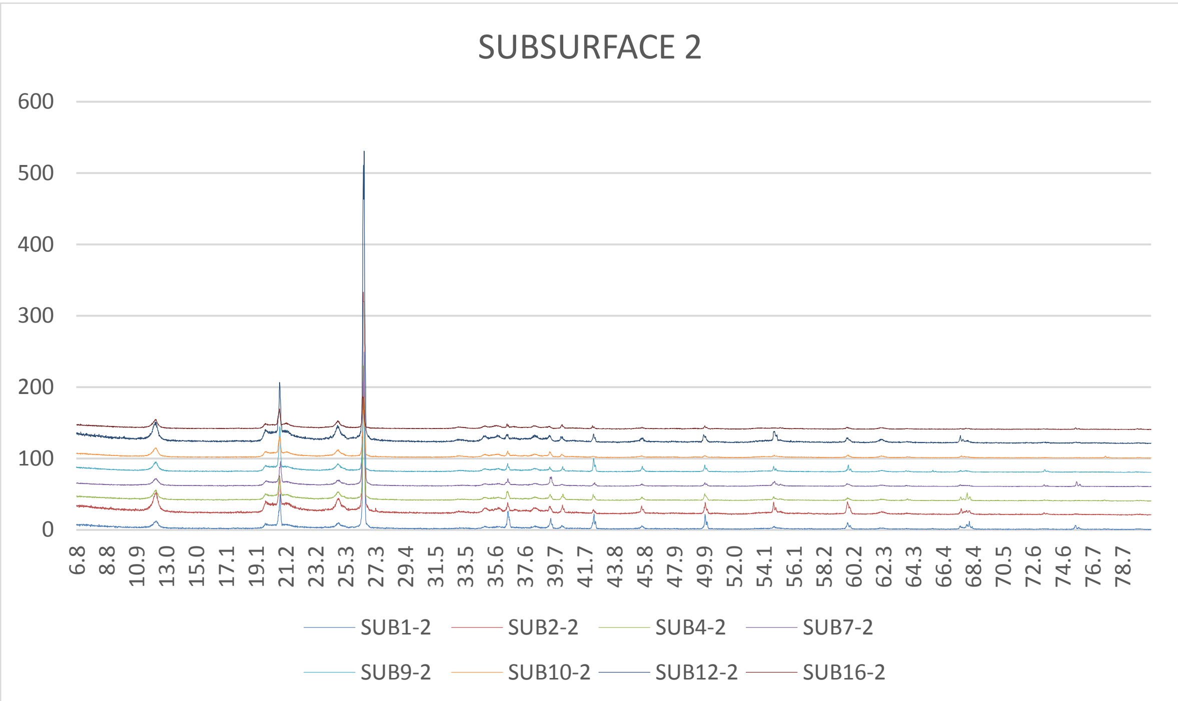

9.5. Appendix 1.4

VNIR-SWIR results from mound 1.

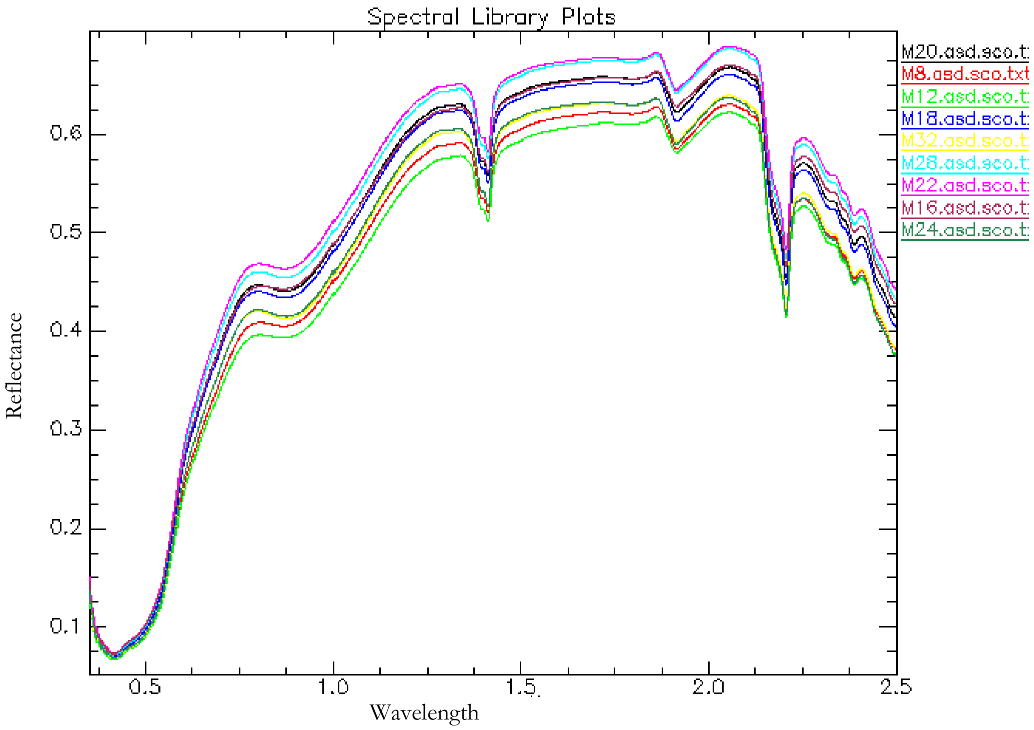

9.6. Appendix 1.5

VNIR-SWIR results from mound 2.

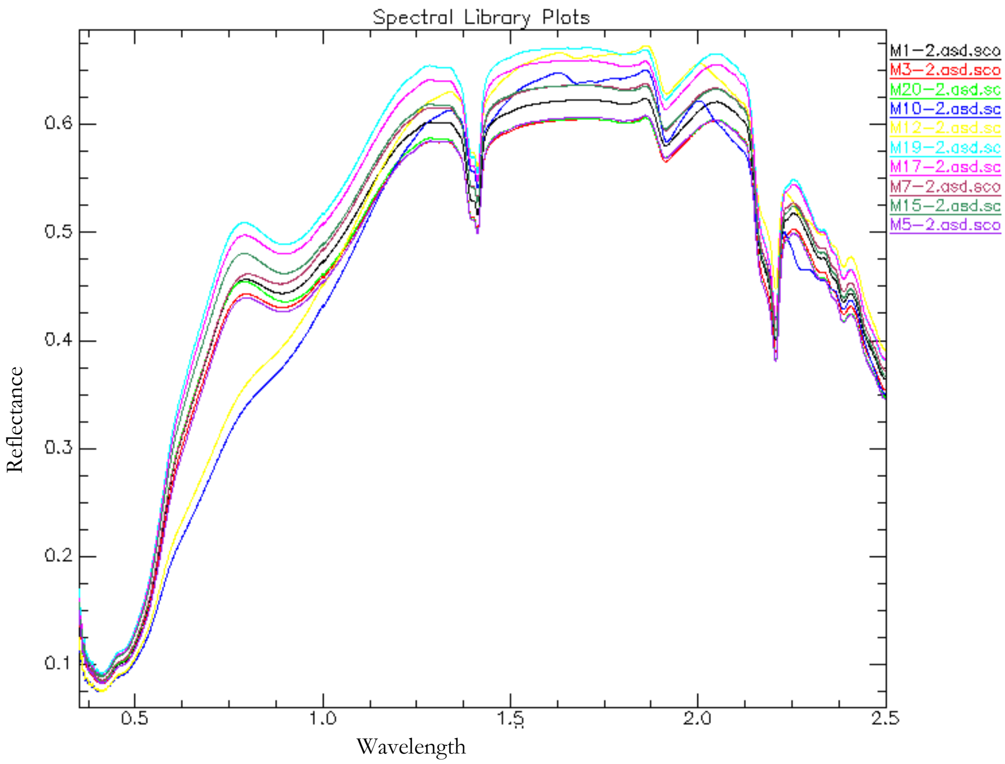

9.7. Appendix 1.6

ICP-OES result of Major and trace elements from the two termite mounds and their immediate subsurface.

Sample Id	Mg (mg/kg)	K (mg/kg)	Zn (mg/kg)	In (mg/kg)	Ca (mg/kg)	Fe (mg/kg)	Al (mg/kg)	Au (mg/kg)
				MOUND 1				
M2	802.32	212.77	34.72	30.81	572.49	40517.84	82367.45	133.29
M8	825.15	375.23	33.78	30.88	462.60	38152.46	77945.91	1.41
M12	809.67	4.04	35.22	30.92	417.30	38300.98	77382.65	138.49
M16	767.78	0.01	32.19	28.17	437.68	36696.51	72842.45	102.67
M18	786.91	0.01	32.95	29.22	436.13	38107.99	76843.29	105.33
M20	815.06	0.01	35.84	31.30	433.77	38895.80	78231.75	123.16
M22	790.93	0.01	33.04	31.11	442.72	36985.05	74214.94	70.92
M24	842.80	0.01	36.27	31.29	521.12	39729.33	79117.37	135.23
M28	841.06	0.01	34.55	31.18	498.15	39955.60	78739.51	123.27
M32	794.16	0.01	35.85	33.60	481.02	39058.06	78409.43	136.53
				SUBSURFACE 1				
Sub1	729.97	1833.43	38.29	25.79	301.90	37131.36	75954.21	13.45
sub3	783.49	2206.73	43.60	28.39	356.92	39049.29	80305.67	130.29
sub 4	419.70	2943.02	16.56	17.21	279.92	19049.75	40072.15	100.65
sub6	840.75	2416.63	35.21	32.96	299.11	45200.79	94371.58	15.28
sub8	922.25	2752.87	39.44	37.02	277.94	46947.09	103876.39	141.76
sub9	885.74	2075.08	35.23	35.36	352.35	44685.87	95133.15	156.38
sub11	972.78	1607.07	37.16	37.67	264.27	48588.41	107467.44	126.70
sub12	969.22	1498.28	40.45	36.76	312.32	48650.66	107520.35	114.97
sub14	910.46	762.08	36.07	35.98	298.09	47449.16	104390.33	96.60
s16(15)	959.23	764.90	41.25	40.87	298.61	49594.37	108691.31	145.55
s17(13)	876.69	365.47	40.72	38.90	310.96	50888.42	107755.38	132.11
SUB 20	959.23	260.51	49.27	38.45	328.14	48530.15	106476.76	116.34
				MOUND 2				
M1-2	906.47	0.01	26.72	31.71	330.45	30765.53	74782.41	111.17
M3-2	878.12	0.01	27.62	29.86	329.20	30094.73	72748.15	101.05
M5-2	973.27	0.01	25.39	27.88	428.74	29090.58	71396.32	117.76
M7-2	863.88	0.01	29.14	31.72	369.99	28826.23	72104.41	117.19
M10-2	901.23	0.01	22.58	23.40	876.81	24838.05	61015.74	1.41
M12-2	912.66	0.01	28.64	26.07	755.20	26154.57	64395.14	68.98
M15-2	825.01	0.01	25.19	28.67	251.10	29788.06	72985.22	86.58
M17-2	875.00	0.01	26.70	32.51	303.64	30217.14	75324.02	118.15
M19-2	899.95	0.01	27.13	34.25	247.98	32087.73	77564.31	4.40
M20-2	823.91	0.01	32.78	33.44	271.49	28229.25	68361.16	82.96
				SUBSURFACE 2				
S1-2	948.74	0.01	27.37	30.30	701.85	29894.58	69682.14	156.16
SUB2-2	866.86	0.01	27.23	29.63	347.93	32875.91	74594.66	108.25
SUB4-2	888.00	0.01	27.88	32.37	317.32	33674.69	77045.07	156.58
S7-2	837.76	0.01	32.52	32.28	224.05	35224.62	79987.73	124.70
SUB9-2	1016.44	0.01	38.96	42.16	181.99	54138.12	116263.26	153.60
SUB10-2	908.81	0.01	40.39	40.76	295.45	57584.05	105896.29	155.15
SUB12-2	922.44	0.01	36.57	38.96	210.23	48233.83	101499.28	129.19
SUB16-2	834.16	0.01	42.44	47.35	258.24	72309.88	112836.27	125.77
S17-2	941.48	0.01	39.57	39.94	282.07	49509.97	104272.10	115.50